



ANNALES
HENRI LEBESGUE

VINCENT PERRIER

DISCRETE DE RHAM COMPLEX
INVOLVING A DISCONTINUOUS
FINITE ELEMENT SPACE FOR
VELOCITIES: THE CASE OF
PERIODIC STRAIGHT
TRIANGULAR AND CARTESIAN
MESHES

COMPLEXES DE DE RHAM DISCRETS
IMPLIQUANT UN ESPACE DISCONTINU
POUR LES VITESSES : LE CAS DES
MAILLAGES PÉRIODIQUES TRIANGULAIRES
DROITS ET CARTÉSIENS

ABSTRACT. — The aim of this article is to derive discontinuous finite elements vector spaces which can be put in a discrete de Rham complex for which the matching between the continuous and discrete cohomology spaces can be proven for periodic meshes.

First, the triangular case is addressed, for which we prove that this property holds for the classical discontinuous finite element space for vectors.

On Cartesian meshes, this result does not hold for the classical discontinuous finite element space for vectors. We then show how to use the de Rham complex found for triangular meshes

for enriching the finite element space on Cartesian meshes in order to recover a de Rham complex, on which the same property is proven.

RÉSUMÉ. — Le but de cet article est de développer des espaces éléments finis pour des espaces de vecteurs discontinus, qui peuvent être mis dans un complexe de de Rham discret pour lequel on peut démontrer une correspondance entre l'espace de cohomologie discret et l'espace de cohomologie continu pour des maillages périodiques.

En premier lieu, le cas triangulaire est abordé, dans lequel on prouve que cette propriété est valide pour l'espace habituel d'approximation des vecteurs.

Sur les maillages cartésiens, la propriété n'est pas valide pour l'espace habituel d'approximation des vecteurs. On montre alors comment utiliser le complexe développé dans le cas triangulaire pour enrichir l'espace éléments finis sur les maillages cartésiens afin de retrouver un complexe de de Rham pour lequel la même propriété est démontrée.

1. Introduction

In this article, we are interested in the de Rham complex on a two dimensional space Ω :

$$(1.1) \quad \Lambda^0(\Omega) \xrightarrow{\quad d \quad} \Lambda^1(\Omega) \xrightarrow{\quad d \quad} \Lambda^2(\Omega),$$

where $\Lambda^k(\Omega)$ is the set of k -differential forms, and d is the exterior derivative. For the sake of simplicity, we suppose that Ω is the two dimensional torus \mathbb{T}^2 .

In the context of partial differential equations, it is usually convenient to translate the multilinear forms of (1.1) in terms of *proxies*. This is achieved by choosing a basis of $\Lambda^1(\Omega)$. If $(\mathbf{e}_1, \mathbf{e}_2)$ is an orthogonal basis, its dual basis is denoted by (dx^1, dx^2) , and this leads usually to the two following situations

- When the basis (dx^1, dx^2) is used for Λ^1 , and $dx^1 \wedge dx^2$ is used for Λ^2 , the exterior derivative between Λ^0 and Λ^1 gives a gradient operator on the proxies. In this case, the 0-forms of (1.1) maps to the set A of the scalar potentials, the 1-forms to a set of vectors \mathbf{B} , and the 2-forms to a set of scalars C . The exterior derivative between A and \mathbf{B} is the gradient, ∇ :

$$\begin{aligned} \nabla : A &\longmapsto \mathbf{B} \\ a &\longmapsto \mathbf{b} = (\partial_x a, \partial_y a)^T \end{aligned}$$

whereas the exterior derivative between \mathbf{B} and C is the rotated divergence (or scalar curl, which is obtained by taking the z component of the classical three dimensional curl)

$$\begin{aligned} \nabla^\perp : \mathbf{B} &\longmapsto C \\ \mathbf{b} &\longmapsto c = -\partial_y b_x + \partial_x b_y, \end{aligned}$$

and the diagram (1.1) can be rewritten in term of proxies as

$$(1.2) \quad A \xrightarrow{\quad \nabla \quad} \mathbf{B} \xrightarrow{\quad \nabla^\perp \quad} C.$$

- When the basis $(-dx^2, dx^1)$ is used for Λ^1 , and $dx^1 \wedge dx^2$ is used for Λ^2 , the exterior derivative between Λ^0 and Λ^1 gives the rotated gradient (which can also be seen as a curl) on the proxies. In this case, the 0-forms of (1.1) maps to the set A of scalars (which may be seen as potential vectors by taking the curl of a vector which would have only a z component), the 1-forms to a set of vectors \mathbf{B} , and the 2-forms to a set of scalars C . The exterior derivative between A and \mathbf{B} is the rotated gradient, ∇^\perp :

$$\begin{aligned}\nabla^\perp : A &\mapsto \mathbf{B} \\ a &\mapsto \mathbf{b} = (-\partial_y a, \partial_x a)^T\end{aligned}$$

whereas the exterior derivative between \mathbf{B} and C is the opposite of the two-dimensional divergence

$$\begin{aligned}\nabla \cdot : \mathbf{B} &\mapsto C \\ \mathbf{b} &\mapsto c = \partial_x \mathbf{b}_x + \partial_y \mathbf{b}_y,\end{aligned}$$

and the diagram (1.1) can be rewritten as

$$(1.3) \quad A \xrightarrow{\nabla^\perp} \mathbf{B} \xrightarrow{-\nabla \cdot} C,$$

For the sake of simplicity, we will address rather the diagram

$$(1.4) \quad A \xrightarrow{\nabla^\perp} \mathbf{B} \xrightarrow{\nabla \cdot} C,$$

A natural question that arises when considering diagrams such as (1.2) and (1.4) is whether the sequence is exact, which can be summarised for (1.2) as:

- Is the kernel of ∇ reduced to 0?
- Is $(\nabla^\perp \cdot)$ full rank?
- Do we have $\text{Range}(\nabla) = \ker(\nabla^\perp \cdot)$?

In general, the answer of the previous questions is “no”, however, it is nearly “yes” in the sense that the dimension of the vectorial spaces $\ker \nabla$, $C/\text{Range}(\nabla^\perp \cdot)$ and $\ker \nabla^\perp \cdot / \text{Range}(\nabla)$ (called the *cohomology spaces*) are finite. Following the Hodge theory, these dimensions equal to the zeroth, first and second Betti numbers (denoted by b_0 , b_1 and b_2), which are characteristics of the topology of the domain Ω . We are interested in this article in two-dimensional periodic domain, namely a torus, for which we have $b_0 = b_2 = 1$ and $b_1 = 2$. Also, $\ker \nabla$ and $C/\text{Range}(\nabla^\perp \cdot)$ match with the uniform functions (which is a one dimensional vector space, and so is consistent with $b_0 = b_2 = 1$), whereas $\ker(\nabla^\perp \cdot) / \text{Range}(\nabla)$ matches with the uniform vectors (which is a two dimensional vector space, so is consistent with $b_1 = 2$).

We are now interested in the discrete counterpart of these properties: once Ω is discretised by a mesh, do we have a discrete counterpart of (1.2) and (1.4)? This indeed exists in the conforming finite element context [AL14]. For example, for triangular meshes, the following discrete version of (1.4) involving the space of continuous finite elements \mathbb{P}_k , the space of Raviart–Thomas finite elements \mathbf{RT}_k and the space of discontinuous finite elements \mathbf{dP}_{k-1}

$$(1.5) \quad \mathbb{P}_{k+1} \xrightarrow{\nabla^\perp} \mathbf{RT}_{k+1} \xrightarrow{\nabla \cdot} \mathbf{dP}_k,$$

whereas a discrete version of (1.2) can also be derived

$$(1.6) \quad \mathbb{P}_{k+1} \xrightarrow{\nabla} \mathbf{N}_{k+1} \xrightarrow{\nabla^\perp} d\mathbb{P}_k,$$

where \mathbf{N}_k is the space of two dimensional triangular Nédélec first species finite elements. Several properties of the discrete diagrams (1.5) and (1.6) are important (see [Arn18, Chapter 5.2.2]):

- *the approximation property*: this property is ensured if the discrete spaces are correctly approximating the continuous spaces.
- *The subcomplex property*: this property is a compatibility property between the discrete complex (1.5) and (1.6), which should be a subcomplex respectively of the continuous complexes (1.4) and (1.2), this means for example for the diagram (1.5), $\nabla^\perp(\mathbb{P}_{k+1}) \subset \mathbf{RT}_{k+1}$ and $\nabla \cdot (\mathbf{RT}_{k+1}) \subset d\mathbb{P}_k$ are ensured.
- *The bounded cochain projection property*: this property means the existence of projection operators, e.g. between the continuous and discrete spaces of (1.5), that commutes with the exterior derivative, and that is bounded. This property is usually not easy to address, as the canonical interpolant are not bounded, see [AFW06, Section 5.4] for an example of construction of a bounded cochain projection in the conformal case.

The second and third properties, combined with an additional approximation property, induce another property, the *isomorphism of cohomology* [Arn18, Theorem 5.1]. Another property, the *gap between harmonic forms* [Arn18, Theorem 5.2] controls the gap between the continuous and discrete harmonic forms. All these properties depend on the definition of the bounded cochain projection, which is not yet defined for the spaces we wish to address, and this is why we focus on a simplified case, the periodic case, for which the cohomology spaces are explicit, and match respectively for their proxies with constant scalar, constant vectors, and constant scalars. In this article, we would like to address the following proposition

PROPOSITION 1.1. — *The discrete cohomology space matches exactly with the continuous one.*

Which is expected to hold for periodic meshes.

The finite element exterior calculus has been thoroughly addressed over the last thirty years, first in the electromagnetism context [Bos88, Bos98, Hip01, Hip02], and then extended to the slightly more abstract Hodge Laplacian problem [AFW06, AFW10], and led to a quite complete theory for conforming finite elements on classical cells (quads, triangles, hexa and tetrahedra) [Arn18]. This type of approximation was extended to polytopal meshes see e.g. [BE14, BE15, Bon14, MBE22] for the “Compatible Discrete Operators” framework or [DPD20] for the “Hybrid High Order” method for citing few of these methods. For the classical discontinuous Galerkin methods, as far as we know, few work was considered see however e.g. [HLX22] for recent advances on this topic for the Hodge Laplacian.

In this article, we are interested in finding a discrete counterpart of (1.2) and (1.4) when Ω is meshed with a triangular mesh or with a Cartesian mesh, and with a particular constraint: we want the space of vectors \mathbf{B} to be discretised with discontinuous finite elements. This constraint is in fact motivated by recent results [Gui09, JP24a],

which suggests that not only the classical discontinuous approximation space on triangles has a structure that allows the preservation of curl constraints for hyperbolic systems, but also that a similar structure exists on quadrangular meshes, see e.g. [JP24b] for the low order quadrangular case. Note that currently, the problem of finding curl or divergence preserving schemes is usually addressed with staggered schemes [Bal01, Bal04, BS99, TD17] (based on the discrete de Rham complex of [Arn18]), which makes the task of limiting for shocks while remaining conservative difficult, because the degrees of freedom are spread on all the entities of the mesh, and also because the notion of local conservation is hard to define.

This article is focused on addressing Proposition 1.1 for these discontinuous approximation spaces, but without addressing bounded cochain projection property, which are complicated to address in the nonconformal case, and out of the scope of this paper. As the approximation is nonconforming, the classical differential operators cannot be considered, and discrete differential operators shall be defined. For the sake of simplicity, we will consider differential operators matching with the derivation in the sense of distributions, leading to approximation spaces that are Cartesian products of approximation spaces on different entities of the mesh, similar to the Hybrid High Order framework [DPD20]. The complexes considered are similar to the ones of [Lic17], but include a lower number of degrees of freedom.

The article is organised as follows. In Section 2, the notations for the mesh and the finite element space and the discrete differential operators are given. Some enumeration properties of the mesh are also proven in this section. Then in Section 3, we recall the results of [Lic17] for a choice of vector finite elements inspired by the conformal case (1.5), (1.6). Then, in Section 4, we prove that if Ω is meshed with triangles and if \mathbf{B} is approximated by the usual discontinuous finite element space, then it can be put in a discrete diagram similar to (1.2) and (1.4) where the space A is approximated by the continuous finite element space. The Proposition 1.1 is proven for this discrete diagram. Then in Section 5, the same problem is addressed for Cartesian meshes. We first prove that Proposition 1.1 fails for $k = 0$ with the classical piecewise constant finite element vector space. Inspired by the diagram that holds on triangles, we prove that by enriching the classical discontinuous finite element space, Proposition 1.1 can be recovered. Section 6 is the conclusion.

2. Notations

2.1. Mesh notations

We denote by \mathcal{P} the set of points of the mesh, by \mathcal{C} the set of cells of the mesh, and by \mathcal{F} the set of the faces of the mesh. For a given entity, for example a cell c , we denote by $\mathcal{F}(c)$ the set of faces neighbouring the cell c , and by $\mathcal{C}(f)$ the set of cells neighbouring the face f .

Each face joining points P and Q is supposed to be oriented, and we denote by \mathbf{n}_f the unit normal to the face $f \in \mathcal{F}$ that is positive, namely such that the angle between the vectors \mathbf{n}_f and \overrightarrow{PQ} is positive. Then the neighbouring cell of this face

such that the normal \mathbf{n}_f is inward is the right cell, and the other is the left cell. If \mathbf{u} is a vector that is discontinuous through the face f , then its jump $[[\cdot]]$ is defined as

$$[[\mathbf{u} \cdot \mathbf{n}_f]] = \mathbf{u}_R \cdot \mathbf{n}_f - \mathbf{u}_L \cdot \mathbf{n}_f,$$

where \mathbf{u}_L is the value on the left and \mathbf{u}_R is the value on the right.

PROPOSITION 2.1 (Triangular mesh of a torus). — *For a triangular mesh, if N denotes the number of cells, then*

$$\begin{cases} \#\mathcal{C} = N \\ \#\mathcal{F} = \frac{3N}{2} \\ \#\mathcal{P} = \frac{N}{2}. \end{cases}$$

Proof. — We remark that the following sum

$$\sum_{f \in \mathcal{F}} \sum_{c \in \mathcal{C}(f)} 1,$$

can be computed in two manners: on one hand, we have two cells per face, so this sum is equal to $2\#\mathcal{F}$. On the other hand, when doing this sum, each cell is visited 3 times (because each cell has three faces), and so the sum is equal to $3N$. This gives $\#\mathcal{F} = \frac{3N}{2}$.

The Euler formula states that

$$\#\mathcal{P} - \#\mathcal{F} + \#\mathcal{C} = 2(1 - g),$$

where g is the genus of the surface. As we are dealing with a two-dimensional domain, with periodic boundary conditions, this is a torus in three dimensions, so that $g = 1$. This leads to

$$\#\mathcal{P} = \#\mathcal{F} - \#\mathcal{C} = \frac{3N}{2} - N = \frac{N}{2}. \quad \square$$

PROPOSITION 2.2 (Cartesian mesh of a torus). — *For a Cartesian mesh with periodicity, if N denotes the number of cells, then*

$$\begin{cases} \#\mathcal{C} = N \\ \#\mathcal{F} = 2N \\ \#\mathcal{P} = N. \end{cases}$$

Proof. — We remark that the following sum

$$\sum_{f \in \mathcal{F}} \sum_{c \in \mathcal{C}(f)} 1,$$

can be computed in two manners: on one hand, we have two cells per face, so this sum is equal to $2\#\mathcal{F}$. On the other hand, when doing this sum, each cell is visited 4 times (because each cell has four faces), and so the sum is equal to $4N$. This means that

$$\#\mathcal{F} = 2N.$$

We are now interested in the following sum

$$\sum_{p \in \mathcal{P}} \sum_{c \in \mathcal{C}(p)} 1,$$

which is both equal to four times the number of points, but also four times the number of cells. This means that $\#\mathcal{P} = N$. \square

2.2. Finite element space notations

In this article, we will consider continuous and discontinuous finite element spaces on faces and cells. We adopt notations close of the ones proposed in [AL14]. We will denote by \mathbb{P}_k the continuous finite element space on triangles. If the finite element space is discontinuous, we will denote it by $\mathrm{d}\mathbb{P}_k$. We will also consider vectorial finite element space, $\mathbf{d}\mathbb{P}_k$. Last, when needed, we will have to consider finite element spaces on entities of the mesh that are not the cells. In this case, we will then denote by a parenthesis indicating on which entity of the mesh the finite element space is defined. For example, $\mathrm{d}\mathbb{P}_k(\mathcal{C})$ is the discontinuous finite element space of degree k defined on the cells, whereas $\mathrm{d}\mathbb{P}_k(\mathcal{F})$ is the discontinuous finite element space of degree k defined on the faces.

The continuous and discontinuous finite element spaces are equipped with the classical L^2 scalar product and its induced norm. In this article, we will also need to deal with Cartesian products of finite element spaces of type $\mathrm{d}\mathbb{P}_i(\mathcal{C}) \times \mathrm{d}\mathbb{P}_j(\mathcal{F})$, on which we will use the following scalar product

$$(2.1) \quad \langle p|q \rangle_{[\mathrm{d}\mathbb{P}_i(\mathcal{C}) \times \mathrm{d}\mathbb{P}_j(\mathcal{F})]} = \sum_{c \in \mathcal{C}} \int_c p_c q_c + \sum_{f \in \mathcal{F}} \int_f p_f q_f.$$

We define the same type of notations by replacing \mathbb{P} by \mathbb{Q} for the case of Cartesian meshes.

On Cartesian meshes, we will use enriched versions of $\mathbf{d}\mathbb{Q}_k$. For this, we define

$$\mathbb{Q}_{i,j} = \left\{ p \in \mathbb{R}[x, y] \quad d_x^\circ p \leq i \quad \text{and} \quad d_y^\circ p \leq j \right\},$$

where d_x° (resp. d_y°) is the degree in x (resp. y), and can define the following cellwise continuous vectorial finite element space on quads

$$(2.2) \quad \widehat{\mathbf{d}\mathbb{Q}_k}^{\mathrm{div}}(\mathcal{C}) = \begin{pmatrix} \mathrm{d}\mathbb{Q}_{k,k} + \mathrm{d}\mathbb{Q}_{k+1,k-1} \\ \mathrm{d}\mathbb{Q}_{k,k} + \mathrm{d}\mathbb{Q}_{k-1,k+1} \end{pmatrix} \oplus \mathrm{Vec} \begin{pmatrix} -x^{k+1}y^k \\ x^ky^{k+1} \end{pmatrix}$$

that will be suited for the curl/div diagram (1.4), and the following vectorial finite element space

$$(2.3) \quad \widehat{\mathbf{d}\mathbb{Q}_k}^{\mathrm{curl}}(\mathcal{C}) = \begin{pmatrix} \mathrm{d}\mathbb{Q}_{k,k} + \mathrm{d}\mathbb{Q}_{k-1,k+1} \\ \mathrm{d}\mathbb{Q}_{k,k} + \mathrm{d}\mathbb{Q}_{k+1,k-1} \end{pmatrix} \oplus \mathrm{Vec} \begin{pmatrix} x^ky^{k+1} \\ x^{k+1}y^k \end{pmatrix}$$

that will be suited for the grad/curl diagram (1.2), and which is nothing but a $\pi/2$ rotation of $\widehat{\mathbf{d}\mathbb{Q}_k}^{\mathrm{div}}(\mathcal{C})$. Note that the space (2.2) is the discontinuous version of the space \mathbf{S}_r defined in [ABF05, p. 2432] for ensuring optimal approximation of vectors on general quadrangular meshes. It is clear that the cellwise divergence of $\widehat{\mathbf{d}\mathbb{Q}_k}^{\mathrm{div}}(\mathcal{C})$ or the cellwise curl of $\widehat{\mathbf{d}\mathbb{Q}_k}^{\mathrm{curl}}(\mathcal{C})$ map to the following finite element space

$$\widehat{\mathbf{d}\mathbb{Q}_{k-1}}(\mathcal{C}) := \mathrm{d}\mathbb{Q}_{k-1}(\mathcal{C}) + \mathrm{d}\mathbb{Q}_{k,k-1}(\mathcal{C}) + \mathrm{d}\mathbb{Q}_{k-1,k}(\mathcal{C}).$$

Last, we will denote by \mathbb{K} the space of constant elements of the discretisation of the space A , \mathbf{K} the space of constant vectors of the discretisation of the space \mathbf{B} and \mathbb{k} the space of constant elements of $d\mathbb{P}_k(\mathcal{F})$.

3. Finite element spaces inspired by the conformal case

In the conformal case, it is known that the Proposition 1.1 is ensured for the following complexes

$$(3.1) \quad \begin{cases} \mathbb{P}_{k+1} \xrightarrow{\nabla^\perp} \mathbf{RT}_{k+1}^\Delta(\mathcal{C}) \xrightarrow{\nabla \cdot} d\mathbb{P}_k(\mathcal{C}) \\ \mathbb{Q}_{k+1} \xrightarrow{\nabla^\perp} \mathbf{RT}_{k+1}^\square(\mathcal{C}) \xrightarrow{\nabla \cdot} d\mathbb{Q}_k(\mathcal{C}) \end{cases},$$

on both the triangular and quadrangular case. The trace of the Raviart–Thomas finite element spaces $\mathbf{RT}_{k+1}^\square$ and \mathbf{RT}_{k+1}^Δ are known to be of degree k in both the triangular and quadrangular case. Therefore, by relaxing the normal continuity constraint, the following complexes may be considered

$$(3.2) \quad \begin{cases} \mathbb{P}_{k+1} \xrightarrow{\nabla^\perp} \mathbf{dRT}_{k+1}^\Delta(\mathcal{C}) \xrightarrow{\nabla_{\mathcal{F}} \cdot} d\mathbb{P}_k(\mathcal{C}) \times d\mathbb{P}_k(\mathcal{F}) \\ \mathbb{Q}_{k+1} \xrightarrow{\nabla^\perp} \mathbf{dRT}_{k+1}^\square(\mathcal{C}) \xrightarrow{\nabla_{\mathcal{F}} \cdot} d\mathbb{Q}_k(\mathcal{C}) \times d\mathbb{P}_k(\mathcal{F}). \end{cases}$$

The discrete maps are defined as follows:

- ∇^\perp is the classical ∇^\perp operator:

$$\forall c \in \mathcal{C} \quad \forall p \in \mathbb{P}_{k+1} \quad \nabla^\perp(p)|_c = \nabla^\perp(p|_c).$$

- $\nabla_{\mathcal{F}} \cdot$ is the divergence where the derivation is taken in the sense of distributions:

$$\forall \mathbf{u} \in \mathbf{dP}_k \quad \begin{cases} \forall c \in \mathcal{C} & \nabla_{\mathcal{F}} \cdot (\mathbf{u})|_c = \nabla \cdot (\mathbf{u}|_c) \\ \forall f \in \mathcal{F} & \nabla_{\mathcal{F}} \cdot (\mathbf{u})|_f = \llbracket \mathbf{u} \cdot \mathbf{n}_f \rrbracket. \end{cases}$$

We first compute the dimension of each of the finite element spaces of (3.2)

PROPOSITION 3.1 (Dimension of the finite element spaces). — *If the mesh is triangular and periodic, then*

$$\begin{cases} \dim \mathbb{P}_{k+1} = \frac{N(k+1)^2}{2} \\ \dim \mathbf{dRT}_{k+1}^\Delta(\mathcal{C}) = N(k+1)(k+3) \\ \dim (d\mathbb{P}_k(\mathcal{F}) \times d\mathbb{P}_k(\mathcal{C})) = \frac{N(k+1)(k+5)}{2}. \end{cases}$$

whereas for a Cartesian periodic mesh,

$$\begin{cases} \dim \mathbb{Q}_{k+1} = N(k+1)^2 \\ \dim \mathbf{dRT}_{k+1}^\square(\mathcal{C}) = 2N(k+2)(k+1) \\ \dim (d\mathbb{P}_k(\mathcal{F}) \times d\mathbb{Q}_k(\mathcal{C})) = N(k+1)(k+3). \end{cases}$$

Proof. — We first address the triangular case. A \mathbb{P}_{k+1} continuous finite element space has

- 1 degree of freedom on each point.
- k degrees of freedom on each face.
- $\frac{k(k-1)}{2}$ degrees of freedom inside each cell.

Adding all these degrees of freedom leads to

$$\begin{aligned} \dim \mathbb{P}_{k+1} &= 1 \times \#\mathcal{P} + k\#\mathcal{F} + \frac{k(k-1)}{2} \#\mathcal{C} \\ &= \frac{N}{2} + k \frac{3N}{2} + \frac{k(k-1)}{2} N \\ &= \frac{N}{2} (1 + 3k + k(k-1)) \\ &= \frac{N}{2} (k^2 + 2k + 1) \\ \dim \mathbb{P}_{k+1} &= \frac{N(k+1)^2}{2}. \end{aligned}$$

Then the $(k+1)^{\text{th}}$ order Raviart–Thomas simplicial finite element is known for having $(k+1)(k+3)$ degrees of freedom (see e.g. [EG20, Lemma 14.6 p. 137]⁽¹⁾). As the space is discontinuous, this gives

$$\dim \mathbf{dRT}_{k+1}^{\triangle} = N(k+1)(k+3).$$

It remains to compute the dimension of $\mathbf{dP}_k(\mathcal{F}) \times \mathbf{dP}_k(\mathcal{C})$

$$\begin{aligned} \dim (\mathbf{dP}_k(\mathcal{F}) \times \mathbf{dP}_k(\mathcal{C})) &= (k+1)\#\mathcal{F} + \frac{(k+1)(k+2)}{2} \#\mathcal{C} \\ &= (k+1) \frac{3N}{2} + \frac{(k+1)(k+2)}{2} N \\ &= \frac{N}{2} (k+1)(k+5). \end{aligned}$$

We are now interested in the dimension of the finite element spaces for the quadrangular mesh. We begin by computing the dimension of \mathbb{Q}_{k+1} . An element of \mathbb{Q}_{k+1} has

- 1 degree of freedom at each point,
- k degrees of freedom at each face,
- k^2 degrees of freedom inside each cell.

Summing all these degrees of freedom and using Proposition 2.2 gives

$$\dim \mathbb{Q}_{k+1} = \#\mathcal{P} + k\#\mathcal{F} + k^2\#\mathcal{C} = N + k(2N) + k^2N = N(k+1)^2.$$

Then the $(k+1)^{\text{th}}$ order Raviart–Thomas quadrangular finite element is known for having $2(k+1)(k+2)$ degrees of freedom (see e.g. [EG20, Section 14.5.2 p. 142]). As the space is discontinuous, this gives

$$\dim \mathbf{dRT}_{k+1}^{\square} = N(k+1)(k+3).$$

⁽¹⁾Note that regarding the notations, what is denoted by $\mathbf{RT}_k^{\triangle}$ in [EG20] is denoted here $\mathbf{RT}_{k+1}^{\triangle}$.

It remains to compute the dimension of $d\mathbb{P}_k(\mathcal{F}) \times d\mathbb{Q}_k(\mathcal{C})$

$$\begin{aligned} \dim(d\mathbb{P}_k(\mathcal{F}) \times d\mathbb{Q}_k(\mathcal{C})) &= (k+1)\#\mathcal{F} + (k+1)^2\#\mathcal{C} \\ &= (k+1)2N + (k+1)^2N \\ &= N(k+1)(k+3). \end{aligned} \quad \square$$

Properties of the complex (3.2) was addressed in a more general framework in [Lic17], and lead in dimension 2 to the following proposition

PROPOSITION 3.2. — *The discrete diagram (3.2) ensures the Proposition 1.1. Moreover, for triangles:*

$$\begin{cases} \mathbb{P}_{k+1}/\mathbb{K} = \ker(\nabla^\perp) \\ (d\mathbb{P}_k(\mathcal{F}) \times d\mathbb{P}_k(\mathcal{C})) / \mathbb{K} = \text{Range}(\nabla_{\mathcal{D}'}) , \end{cases}$$

and for quadrangles

$$\begin{cases} \mathbb{Q}_{k+1}/\mathbb{K} = \ker(\nabla^\perp) \\ (d\mathbb{P}_k(\mathcal{F}) \times d\mathbb{Q}_k(\mathcal{C})) / \mathbb{K} = \text{Range}(\nabla_{\mathcal{D}'}) . \end{cases}$$

The location of the degrees of freedom for this discrete de Rham complex for Cartesian meshes is summarised in Figure 3.1, and in Figure 3.3 for triangles.

By changing the representation of the linear forms, which is equivalent to rotating of $\pi/2$ the vector spaces, the following proposition is also obtained:

PROPOSITION 3.3. — *The discrete diagram*

$$\begin{cases} \mathbb{P}_{k+1} \xrightarrow{\nabla} \mathbf{dN}_{k+1}^\Delta(\mathcal{C}) \xrightarrow{\nabla_{\mathcal{D}'}^\perp} d\mathbb{P}_k(\mathcal{C}) \times d\mathbb{P}_k(\mathcal{F}) \\ \mathbb{Q}_{k+1} \xrightarrow{\nabla} \mathbf{dN}_{k+1}^\square(\mathcal{C}) \xrightarrow{\nabla_{\mathcal{D}'}^\perp} d\mathbb{Q}_k(\mathcal{C}) \times d\mathbb{P}_k(\mathcal{F}). \end{cases}$$

where $\nabla_{\mathcal{D}'}^\perp \cdot$ is $\nabla^\perp \cdot$ in the sense of distributions, ensures the Proposition 1.1. Moreover, for triangles:

$$\begin{cases} \mathbb{P}_{k+1}/\mathbb{K} = \ker(\nabla) \\ (d\mathbb{P}_k(\mathcal{F}) \times d\mathbb{P}_k(\mathcal{C})) / \mathbb{K} = \text{Range}(\nabla_{\mathcal{D}'}^\perp) , \end{cases}$$

and for quadrangles

$$\begin{cases} \mathbb{Q}_{k+1}/\mathbb{K} = \ker(\nabla) \\ (d\mathbb{P}_k(\mathcal{F}) \times d\mathbb{Q}_k(\mathcal{C})) / \mathbb{K} = \text{Range}(\nabla_{\mathcal{D}'}^\perp) . \end{cases}$$

The location of the degrees of freedom for this discrete de Rham complex for Cartesian meshes is summarised in Figure 3.2 and in Figure 3.4 for triangles.

In this section, results of [Lic17] for discontinuous finite element spaces for vectors have been recalled to ensure the Proposition 1.1. Still, as the spaces **dRT** and **dN** are obtained by relaxing the normal continuity constraint of the classical conformal finite element spaces **RT** and **N**, their number of degrees of freedom are not optimal. In the following sections, we will try to develop vector finite element spaces with a lower number of degrees of freedom for which the Proposition 1.1 holds also, by beginning by the triangular meshes case.

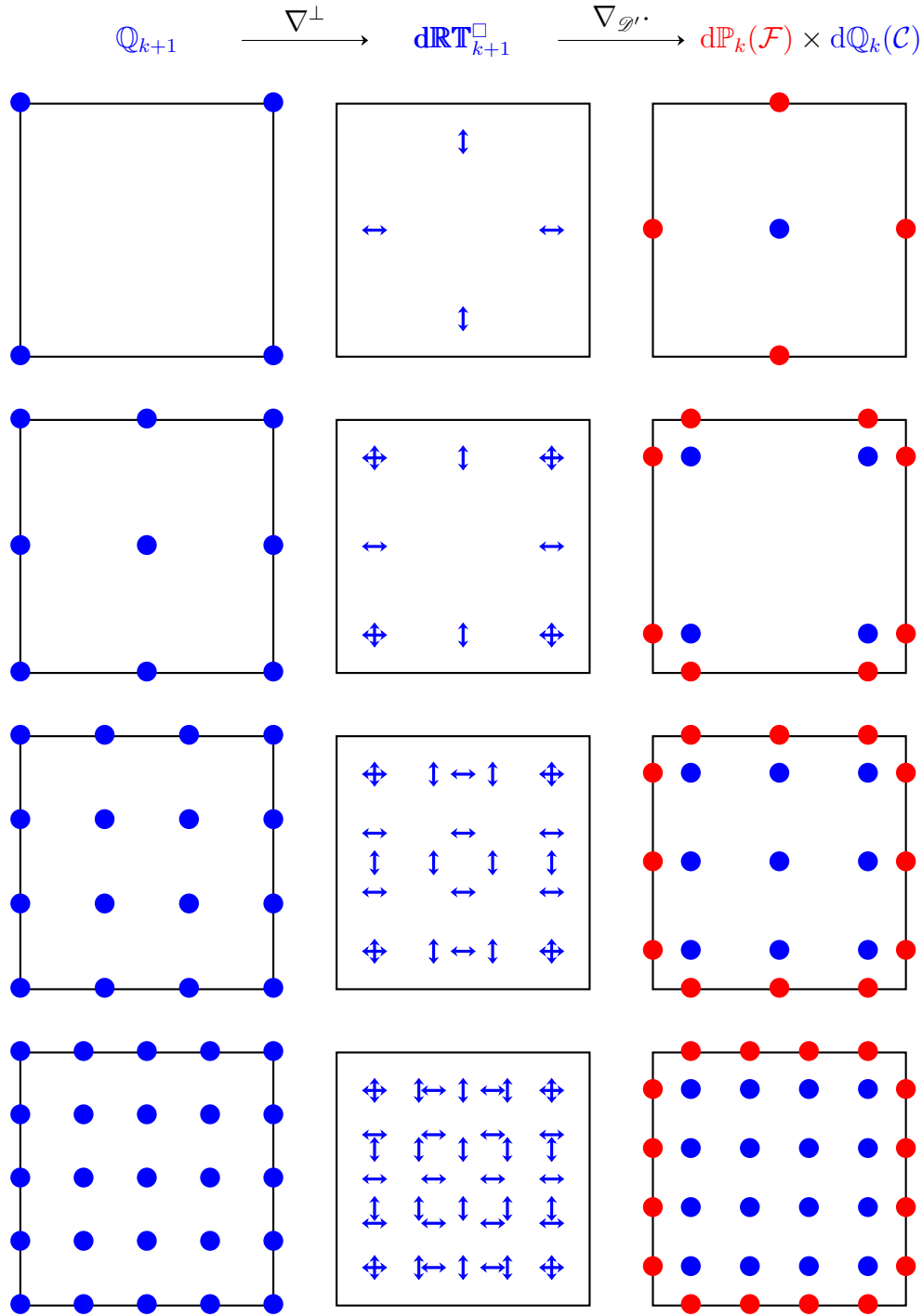


Figure 3.1. Representation of the degrees of freedom of the finite element spaces involved in the curl/div de Rham complex for Cartesian meshes for $k = 0, 1, 2$ and 3 . Points denote scalar degrees of freedom, whereas arrows denote vectorial degrees of freedom. Both scalar and vectorial volume degrees of freedom are represented in blue, whereas the degrees of freedom in the face finite element space are represented in red.

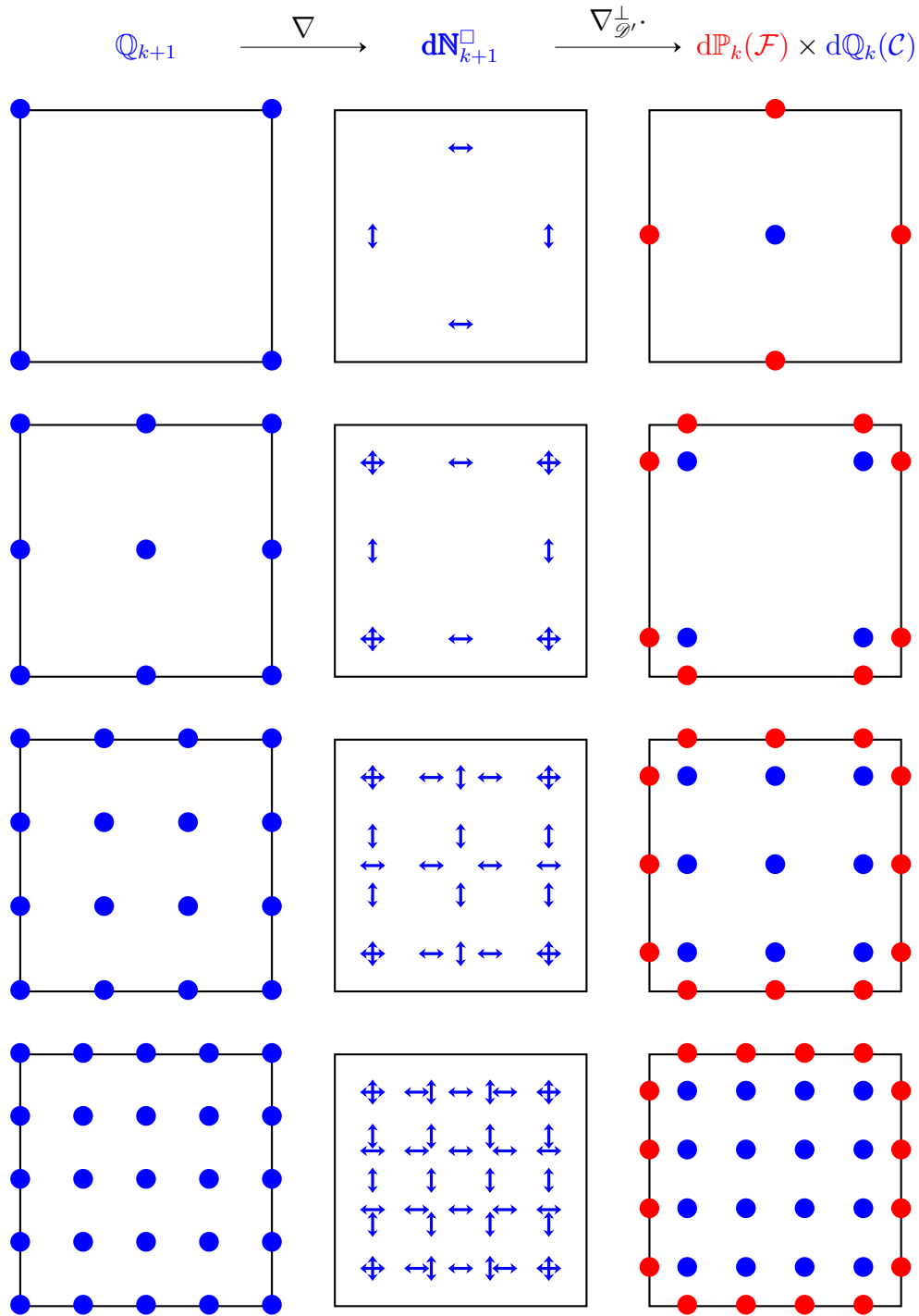


Figure 3.2. Representation of the degrees of freedom of the finite element spaces involved in the grad/curl de Rham complex for Cartesian meshes for $k = 0, 1, 2$ and 3 . Same code for colors as in Figure 3.1 is used.

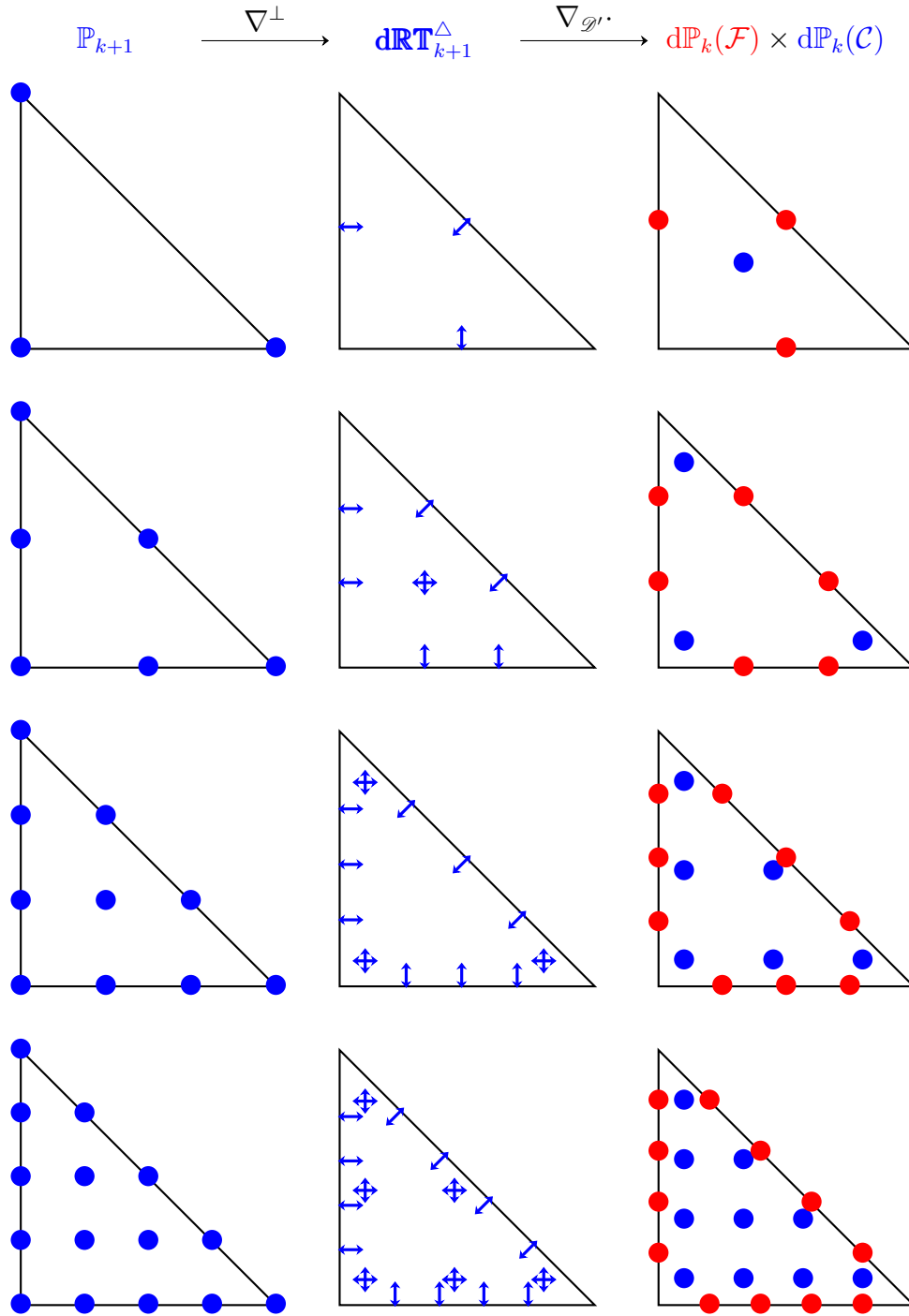


Figure 3.3. Representation of the finite element spaces involved in the curl/div de-Rham complex for triangular meshes for $k = 0, 1, 2$ and 3 . Same code for colors as in Figure 3.1 is used.

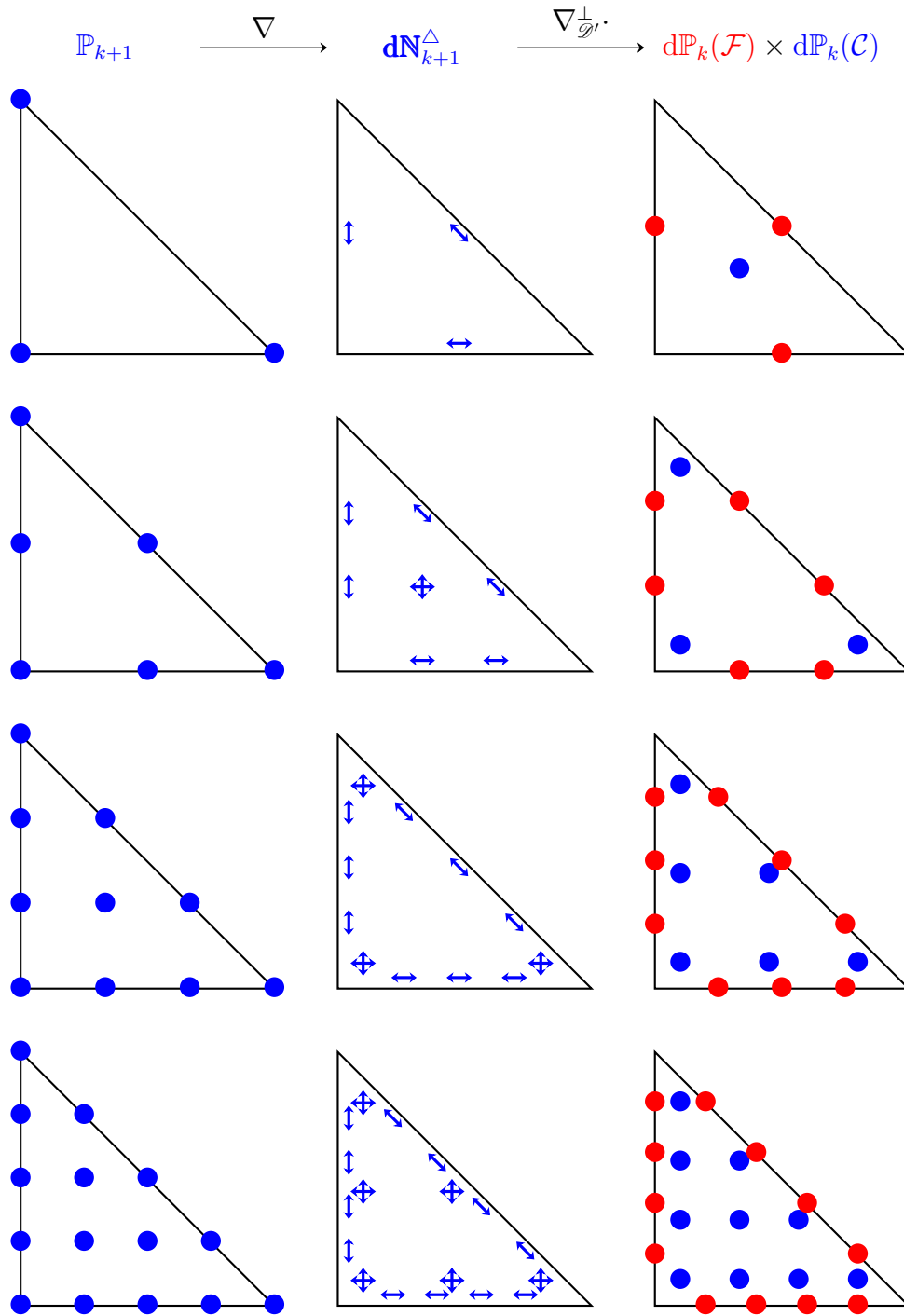


Figure 3.4. Representation of the finite element spaces involved in the grad/curl de-Rham complex for triangular meshes for $k = 0, 1, 2$ and 3 . Same code for as in Figure 3.1 is used.

4. The triangular mesh case

In this section, we are interested in the following diagram

$$(4.1) \quad \mathbb{P}_{k+1} \xrightarrow{\nabla^\perp} \mathbf{dP}_k(\mathcal{C}) \xrightarrow{\nabla_{\mathcal{D}'}} \mathbf{dP}_k(\mathcal{F}) \times \mathbf{dP}_{k-1}(\mathcal{C}).$$

4.1. Dimension of the finite elements spaces

We first compute the dimension of each of the finite element spaces involved in (4.1), induced by the number of faces, points and cells that was computed in Proposition 2.1.

PROPOSITION 4.1 (Dimension of the finite element spaces). — *If the mesh is triangular and periodic, then*

$$\begin{cases} \dim \mathbb{P}_{k+1} = \frac{N(k+1)^2}{2} \\ \dim \mathbf{dP}_k(\mathcal{C}) = N(k+1)(k+2) \\ \dim (\mathbf{dP}_k(\mathcal{F}) \times \mathbf{dP}_{k-1}(\mathcal{C})) = \frac{(k+1)(k+3)N}{2}. \end{cases}$$

Proof. — The dimension of \mathbb{P}_{k+1} was already proven in Proposition 3.1. We are now interested in the dimension of $\mathbf{dP}_k(\mathcal{C})$. This space is a vector space, and so is composed of two components, each of these components having $\frac{(k+1)(k+2)}{2}$ degrees of freedom on each cell. This gives

$$\dim \mathbf{dP}_k(\mathcal{C}) = 2N \times \frac{(k+1)(k+2)}{2} = N(k+1)(k+2).$$

We are finally interested in the dimension of $\mathbf{dP}_k(\mathcal{F}) \times \mathbf{dP}_{k-1}(\mathcal{C})$. This finite element space includes $k+1$ degrees of freedom on each face, and $\frac{k(k+1)}{2}$ degrees of freedom on each cell. Adding all these degrees of freedom leads to

$$\begin{aligned} \dim (\mathbf{dP}_k(\mathcal{F}) \times \mathbf{dP}_{k-1}(\mathcal{C})) &= (k+1)\#\mathcal{F} + \frac{k(k+1)}{2}\#\mathcal{C} \\ &= (k+1)\frac{3N}{2} + \frac{k(k+1)}{2}N \\ \dim (\mathbf{dP}_k(\mathcal{F}) \times \mathbf{dP}_{k-1}(\mathcal{C})) &= \frac{(k+1)(k+3)N}{2}, \end{aligned}$$

which ends the proof of this proposition. \square

4.2. Study of ∇^\perp

We are now interested in the study of the ∇^\perp operator.

PROPOSITION 4.2 (∇^\perp in the triangular case). — We have

$$\begin{cases} \dim(\ker \nabla^\perp) = 1 \\ \text{rank}(\nabla^\perp) = \frac{N(k+1)^2}{2} - 1. \end{cases}$$

Proof. — Suppose that a $\psi \in \mathbb{P}_{k+1}$ is such that $\nabla^\perp \psi = 0$. Then $\partial_x \psi = \partial_y \psi = 0$, so that ψ is piecewise constant. But as ψ is continuous, it is actually uniform:

$$\ker \nabla^\perp = \mathbb{K}.$$

This gives $\dim \ker \nabla^\perp = 1$, as we are working on a domain with a single connected component. Applying the rank-nullity theorem in the triangular case

$$\dim \mathbb{P}_k = \dim \ker \nabla^\perp + \text{rank}(\nabla^\perp),$$

leads to

$$\text{rank}(\nabla^\perp) = \dim \mathbb{P}_k - 1 = \frac{N(k+1)^2}{2} - 1.$$

In the same manner, we get, in the quadrangular case:

$$\text{rank}(\nabla^\perp) = N(k+1)^2 - 1. \quad \square$$

4.3. Discrete divergence free polynomials on the reference cell

We consider the following application

$$(4.2) \quad \mathbf{C}_k^\partial : \psi \in \text{d}\mathbb{P}_{k+1}(\widehat{K}) \longmapsto \mathbf{Tr}(\nabla^\perp \psi) \in \text{d}\mathbb{P}_k(\partial \widehat{K}),$$

where \widehat{K} is the reference triangle.

PROPOSITION 4.3. — We denote by \mathbb{k} the constant elements of $\text{d}\mathbb{P}_k(\partial \widehat{K})$. Then

$$\text{d}\mathbb{P}_k(\partial \widehat{K}) = \text{Range } \mathbf{C}_k^\partial \oplus \mathbb{k},$$

where the sum is orthogonal.

Proof. — We denote by c an element of \mathbb{k} . We denote also by c the function equal to c on \widehat{K} . We also denote by u an element of $\text{Range } \mathbf{C}^\partial$. Then a ψ exists such that $u = \mathbf{C}_k^\partial(\psi)$. Then

$$\begin{aligned} \int_{\partial \widehat{K}} uc &= \int_{\partial \widehat{K}} \mathbf{Tr}(\nabla^\perp \psi) c \\ &= \int_{\widehat{K}} \nabla \cdot (c \nabla^\perp \psi) \\ &= \int_{\widehat{K}} c \nabla \cdot (\nabla^\perp \psi) + \int_{\widehat{K}} \nabla c \cdot \nabla^\perp \psi \\ \int_{\partial \widehat{K}} uc &= 0, \end{aligned}$$

because c is constant and $\nabla \cdot (\nabla^\perp \psi) = 0$. We thus have proven that the sum

$$\text{Range } \mathbf{C}_k^\partial + \mathbb{k},$$

is direct and orthogonal.

We are now interested in the study of the kernel of \mathbf{C}_k^∂ . Suppose that an element ψ is such that $\mathbf{C}_k^\partial(\psi) = 0$. We consider the classical Lagrange basis of $\mathbf{dP}_{k+1}(\widehat{K})$. Then ψ is such that its value on the boundary of \widehat{K} is constant, and may take any value on the degrees of freedom matching with the interior nodes. This means that

$$\dim(\ker \mathbf{C}_k^\partial) = 1 + \frac{k(k-1)}{2}.$$

Using the rank-nullity theorem gives

$$\begin{aligned} \text{rank}(\mathbf{C}_k^\partial) &= \dim \mathbf{dP}_{k+1} - \left(1 + \frac{k(k-1)}{2}\right) \\ &= \frac{(k+2)(k+3)}{2} - 1 - \frac{k(k-1)}{2} \\ &= \frac{k^2 + 5k + 6 - k^2 + k - 2}{2} \\ &= \frac{6k + 4}{2} \\ \text{rank}(\mathbf{C}_k^\partial) &= 3k + 2. \end{aligned}$$

We also know that $\dim \mathbf{dP}_k(\partial \widehat{K}) = 3(k+1)$. We have then $\text{Range } \mathbf{C}_k^\partial \oplus \mathbb{k} \subset \mathbf{dP}_k(\partial \widehat{K})$, and $\dim(\text{Range } \mathbf{C}_k^\partial \oplus \mathbb{k}) = \dim \mathbf{dP}_k(\partial \widehat{K})$, so that $\text{Range } \mathbf{C}_k^\partial \oplus \mathbb{k} = \mathbf{dP}_k(\partial \widehat{K})$, which ends the proof. \square

PROPOSITION 4.4 (Decomposition of divergence free elements). — We denote by $\mathcal{L}^{f,i}$ the Legendre polynomial of degree i on the face f of \widehat{K} , normalised such that

$$\int_{\partial \widehat{K}} (\mathcal{L}^{f,i})^2 = 1.$$

Suppose that $\mathbf{u} \in \mathbf{dP}_k(\widehat{K})$ is divergence free. Then \mathbf{u} can be uniquely decomposed as

$$(4.3) \quad \mathbf{u} = \bar{\mathbf{v}}_{\mathbf{u}}^0 + \bar{\mathbf{v}}_{\mathbf{u}}^1 + \sum_{f \in \mathcal{F}(\widehat{K})} \sum_{i=1}^k \bar{\mathbf{v}}_{\mathbf{u}}^{f,i},$$

where

- $\bar{\mathbf{v}}_{\mathbf{u}}^0$ is in the set

$$\Phi_k = \{\mathbf{u} \in \mathbf{dP}_k \quad \nabla \cdot \mathbf{u} = 0 \quad \text{Tr}(\mathbf{u}) = 0\}.$$

- $\bar{\mathbf{v}}_{\mathbf{u}}^1$ is constant.
- $\bar{\mathbf{v}}_{\mathbf{u}}^{f,i}$ is orthogonal to Φ_k and such that
 - $\nabla \cdot \bar{\mathbf{v}}_{\mathbf{u}}^{f,i} = 0$.
 - $\text{Tr}(\bar{\mathbf{v}}_{\mathbf{u}}^{f,i})$ is orthogonal to all $\mathcal{L}^{g,j}$ for $\{g,j\} \neq \{f,i\}$.

Note that the sum over the integers i in the sum of $\bar{\mathbf{v}}_{\mathbf{u}}^{f,i}$ in (4.3) begins at 1 and not 0 for excluding the ones that would have a constant trace. Note also that the set Φ_k is the same as in the decomposition used in [BF91, Proposition 3.1] for the derivation

of classical conformal divergence free finite elements of Raviart–Thomas [RT77a, RT77b] or Brezzi–Douglas–Marini [BDM85] types (these are respectively referred as *RT* and *BDM* in [AL14]).

Proof. — We first prove that $\bar{\mathbf{v}}_{\mathbf{u}}^1$, if it exists, is orthogonal to Φ_k . We denote by \mathbf{u}_Φ an element of Φ_k . Then a ψ^Φ exists such that $\mathbf{u}_\Phi = \nabla^\perp \Psi^\Phi$. As $\mathbf{u}_\Phi \in \Phi_k$, Ψ^Φ is constant on $\partial\widehat{K}$. Then

$$\begin{aligned} \int_{\widehat{K}} \bar{\mathbf{v}}_{\mathbf{u}}^1 \cdot \mathbf{u}_\Phi &= \int_{\widehat{K}} \bar{\mathbf{v}}_{\mathbf{u}}^1 \cdot \nabla^\perp \Psi^\Phi \\ &= \int_{\widehat{K}} \left(\bar{\mathbf{v}}_{\mathbf{u}}^1 \right)^\perp \cdot \nabla \Psi^\Phi \\ &= \int_{\widehat{K}} \nabla \cdot \left(\left(\bar{\mathbf{v}}_{\mathbf{u}}^1 \right)^\perp \Psi^\Phi \right) \\ &= \int_{\partial\widehat{K}} \mathbf{Tr} \left(\left(\bar{\mathbf{v}}_{\mathbf{u}}^1 \right)^\perp \Psi^\Phi \right) \\ \int_{\widehat{K}} \bar{\mathbf{v}}_{\mathbf{u}}^1 \cdot \mathbf{u}_\Phi &= 0, \end{aligned}$$

because both $\left(\bar{\mathbf{v}}_{\mathbf{u}}^1 \right)^\perp$ and Ψ^Φ are constant on $\partial\widehat{K}$. We have then proven that $\bar{\mathbf{v}}_{\mathbf{u}}^1 \perp \Phi_k$.

We can now prove the uniqueness of the decomposition. We suppose that

$$0 = \bar{\mathbf{v}}_{\mathbf{u}}^0 + \bar{\mathbf{v}}_{\mathbf{u}}^1 + \sum_{f \in \mathcal{F}(\widehat{K})} \sum_{i=1}^k \bar{\mathbf{v}}_{\mathbf{u}}^{f,i},$$

where the different components ensure the properties of the proposition. By definition, $\bar{\mathbf{v}}_{\mathbf{u}}^0$ is orthogonal to the $\bar{\mathbf{v}}_{\mathbf{u}}^{f,i}$, and we proved that it is also orthogonal to $\bar{\mathbf{v}}_{\mathbf{u}}^1$, so that it vanishes. We take the trace of the remaining part, which gives

$$0 = \mathbf{Tr} \left(\bar{\mathbf{v}}_{\mathbf{u}}^1 \right) + \sum_{f \in \mathcal{F}(\widehat{K})} \sum_{i=1}^k \mathbf{Tr} \left(\bar{\mathbf{v}}_{\mathbf{u}}^{f,i} \right).$$

Taking the scalar product by any $\mathcal{L}^{g,j}$ for $j \geq 1$ gives

$$\int_{\partial\widehat{K}} \mathbf{Tr} \left(\bar{\mathbf{v}}_{\mathbf{u}}^{g,j} \right) \mathcal{L}^{g,j} = 0.$$

As $\mathbf{Tr}(\bar{\mathbf{v}}_{\mathbf{u}}^{g,j})$ has a moment only on face g for degree j , it is actually zero. As it is orthogonal to Φ_k , we get $\bar{\mathbf{v}}_{\mathbf{u}}^{g,j} = 0$ for all g, j . It remains then $\bar{\mathbf{v}}_{\mathbf{u}}^1 = 0$, and so each component is zero, which proves the uniqueness of the decomposition.

We now prove the existence. We consider one $\mathcal{L}^{f,i}$ of $\mathbf{dP}_k(\partial\widehat{K})$, for $i \geq 1$. $\mathcal{L}^{f,i}$ is orthogonal to \mathbb{k} , and so using Proposition 4.3, $\mathcal{L}^{f,i}$ is in $\text{Range } \mathbf{C}_k^\partial$, so that a $\psi^{f,i}$ exists such that $\mathbf{C}_k^\partial(\psi^{f,i}) = \mathcal{L}^{f,i}$. Denoting by \mathcal{P} the orthogonal projection on Φ_k , we define $\mathbf{e}^{f,i} := \nabla^\perp(\psi^{f,i}) - \mathcal{P}(\nabla^\perp(\psi^{f,i}))$. Then $\mathbf{e}^{f,i}$ is orthogonal to Φ_k , is divergence free, and is such that $\mathbf{Tr}(\mathbf{e}^{f,i}) = \mathcal{L}^{f,i}$. We consider one divergence free $\mathbf{u} \in \mathbf{dP}_k(\widehat{K})$. We define

$$\lambda_{f,i} := \int_{\partial\widehat{K}} \mathbf{Tr}(\mathbf{u}) \mathcal{L}^{f,i},$$

and set $\bar{\mathbf{v}}_{\mathbf{u}}^{f,i} = \lambda_{f,i} \mathbf{e}^{f,i}$. We also set $\bar{\mathbf{v}}_{\mathbf{u}}^0 = \mathcal{P}(\mathbf{u})$, and

$$\bar{\mathbf{v}}_{\mathbf{u}}^1 := \mathbf{u} - \bar{\mathbf{v}}_{\mathbf{u}}^0 - \sum_{f \in \mathcal{F}(\hat{K})} \sum_{i=1}^k \bar{\mathbf{v}}_{\mathbf{u}}^{f,i}.$$

Then $\bar{\mathbf{v}}_{\mathbf{u}}^0$ and the $\bar{\mathbf{v}}_{\mathbf{u}}^{f,i}$ ensure all the properties required. It remains to prove that $\bar{\mathbf{v}}_{\mathbf{u}}^1$ is constant. We know that $\bar{\mathbf{v}}_{\mathbf{u}}^1$ is divergence free, orthogonal to Φ_k , and that its trace is constant on each face, because all the components in $\mathcal{L}^{f,i}$ for $i \geq 1$ were removed. We denote by \mathbf{k}_y the opposite of the trace on the side linking $[0, 0]$ to $[0, 1]$, and \mathbf{k}_x the opposite of the trace on the side linking $[0, 0]$ to $[1, 0]$, and consider $\mathbf{k} = (\mathbf{k}_x, \mathbf{k}_y)$. As $\nabla \cdot \bar{\mathbf{v}}_{\mathbf{u}}^1 = 0$, we have

$$\begin{aligned} 0 &= \int_{\hat{K}} \nabla \cdot \bar{\mathbf{v}}_{\mathbf{u}}^1 \\ &= \int_{\partial \hat{K}} \text{Tr}(\bar{\mathbf{v}}_{\mathbf{u}}^1) \\ &= \int_{(0,0)}^{(1,0)} \text{Tr}(\bar{\mathbf{v}}_{\mathbf{u}}^1) + \int_{(1,0)}^{(1,1)} \text{Tr}(\bar{\mathbf{v}}_{\mathbf{u}}^1) + \int_{(1,1)}^{(0,0)} \text{Tr}(\bar{\mathbf{v}}_{\mathbf{u}}^1) \\ &= -\mathbf{k}_x - \mathbf{k}_y + \int_{(1,0)}^{(1,1)} \text{Tr}(\bar{\mathbf{v}}_{\mathbf{u}}^1) \\ 0 &= -\mathbf{k}_x - \mathbf{k}_y + \sqrt{2} \text{Tr}(\bar{\mathbf{v}}_{\mathbf{u}}^1)_{|[(1,0),(1,1)]}, \end{aligned}$$

which means that the trace on the side linking $[1, 0]$ to $[1, 1]$ is equal to $\frac{1}{\sqrt{2}}(\mathbf{k}_x + \mathbf{k}_y)$, which is also equal to the trace of \mathbf{k} . This means $\bar{\mathbf{v}}_{\mathbf{u}}^1 - \mathbf{k}$ is divergence free, and that $\text{Tr}(\bar{\mathbf{v}}_{\mathbf{u}}^1 - \mathbf{k}) = 0$, and so $\bar{\mathbf{v}}_{\mathbf{u}}^1 - \mathbf{k} \in \Phi_k$.

As \mathbf{k} is orthogonal to Φ_k , and so is $\bar{\mathbf{v}}_{\mathbf{u}}^1$, we conclude that $\bar{\mathbf{v}}_{\mathbf{u}}^1 - \mathbf{k}$ is also orthogonal to Φ_k . This gives $\bar{\mathbf{v}}_{\mathbf{u}}^1 - \mathbf{k} = 0$, and $\bar{\mathbf{v}}_{\mathbf{u}}^1$ is therefore constant. \square

It is important to note that the decomposition of Proposition 4.4 was proven on the reference element. However, all the properties of the different spaces are invariant by linear transformations. This means that the decomposition of Proposition 4.4 holds actually on any straight triangular cell of the mesh.

4.4. $\ker(\nabla_{\mathcal{D}'})$ and $\text{Range}(\nabla^\perp)$

PROPOSITION 4.5. — *If \mathbb{K} denotes the set of uniform vectors, then*

$$\ker(\nabla_{\mathcal{D}'}) = \text{Range}(\nabla^\perp) \oplus \mathbb{K}.$$

Proof. — We begin by proving that $\text{Range}(\nabla^\perp) \subset \ker(\nabla_{\mathcal{D}'})$. We consider an element \mathbf{u} of $\text{Range}(\nabla^\perp)$. Then a $\Psi \in \mathbb{P}_{k+1}$ exists such that $\mathbf{u} = \nabla^\perp \psi$. Then

$$\forall c \in \mathcal{C} \quad \nabla \cdot (\nabla^\perp \psi) = 0.$$

Also, as ψ is continuous, the jump of $\nabla^\perp \psi$ across faces vanishes. We have then proven that $\text{Range}(\nabla^\perp) \subset \ker(\nabla_{\mathcal{D}'})$.

We now prove that $\text{Range}(\nabla^\perp) \perp \mathbb{K}$. We denote by $\mathbf{k} = (\mathbf{k}_x, \mathbf{k}_y)^T \in \mathbb{K}$, and by ψ an element of \mathbb{P}_k . Then

$$\mathbf{k} \cdot \nabla^\perp \psi = \begin{pmatrix} \mathbf{k}_x \\ \mathbf{k}_y \end{pmatrix} \cdot \begin{pmatrix} -\partial_y \psi \\ \partial_x \psi \end{pmatrix} = -\mathbf{k}_x \partial_y \psi + \mathbf{k}_y \partial_x \psi = \begin{pmatrix} \mathbf{k}_y \\ -\mathbf{k}_x \end{pmatrix} \cdot \nabla \psi.$$

We denote by $\mathbf{k}^\perp = (\mathbf{k}_y, -\mathbf{k}_x)^T$. Then as \mathbf{k}^\perp is uniform, we have on all cells:

$$\nabla \cdot (\mathbf{k}^\perp \psi) = \mathbf{k}^\perp \cdot \nabla \psi.$$

Then

$$\begin{aligned} \sum_{c \in \mathcal{C}} \int_c \mathbf{k}^\perp \cdot \nabla \psi &= \sum_{c \in \mathcal{C}} \int_c \nabla \cdot (\mathbf{k}^\perp \psi) \\ &= \sum_{c \in \mathcal{C}} \int_{\partial c} \psi \mathbf{k}^\perp \cdot \mathbf{n}_{out} \\ &= \sum_{c \in \mathcal{C}} \sum_{f \in \mathcal{F}(c)} \int_f \psi \mathbf{k}^\perp \cdot \mathbf{n}_{out} \\ &= - \sum_f \int_f \llbracket \psi \mathbf{k}^\perp \cdot \mathbf{n}_f \rrbracket \\ \sum_{c \in \mathcal{C}} \int_c \mathbf{k}^\perp \cdot \nabla \psi &= 0, \end{aligned}$$

because both \mathbf{k}^\perp and ψ are continuous across the faces. We have then proven that

$$\mathbb{K} \perp \text{Range}(\nabla^\perp).$$

We also remark that $\mathbb{K} \subset \ker(\nabla_{\mathcal{D}'})$, because $\nabla_{\mathcal{D}'}$ is a derivation operator. For the moment, we have proven that

$$\text{Range}(\nabla^\perp) \oplus \mathbb{K} \subset \ker \nabla_{\mathcal{D}'}$$

Suppose now that an element $\mathbf{u} \in \mathbf{dP}_k$ is such that its divergence is 0, namely

$$\begin{cases} \forall c \in \mathcal{C} & \nabla \cdot \mathbf{u} = 0 \\ \forall f \in \mathcal{F} & \llbracket \mathbf{u} \cdot \mathbf{n}_f \rrbracket = 0. \end{cases}$$

As $\nabla \cdot \mathbf{u} = 0$ on all the cells, \mathbf{u} can be decomposed as in Proposition 4.4; this decomposition involves three types of components:

- The ones of Φ_k , which have a trace equal to 0. This set is of dimension $\frac{k(k-1)}{2}$ on each cell.
- The constant component; this set is of dimension 2 on each cell.
- The components $\bar{\mathbf{v}}_i^f$ for $1 \leq i \leq k$ and for all faces. This set is of dimension $3k$ on each cell.

Let us see now what is the effect of the constraint $\llbracket \mathbf{u} \cdot \mathbf{n}_f \rrbracket = 0$ on these different components. We first remark that the traces of the different components are orthogonal two at a time, which means that we can consider the effect of $\llbracket \mathbf{u} \cdot \mathbf{n}_f \rrbracket = 0$ component by component:

- The ones of Φ_k are not affected by the zero jump constraint, because their trace is already equal to 0. This induces $N \frac{k(k-1)}{2}$ components in \mathbf{dP}_k .

- The piecewise constant components, with the constraint $\llbracket \mathbf{u} \cdot \mathbf{n}_f \rrbracket = 0$ is a set that was already identified in previous publications [AF89, DJOR16, JP22], and this space is $\nabla^\perp \mathbb{P}_1 \oplus \mathbb{K}$, which is of dimension $1 + \frac{N}{2}$.
- Concerning the components $\bar{\mathbf{v}}_i^f$ for $1 \leq i \leq k$, the constraint $\llbracket \mathbf{u} \cdot \mathbf{n}_f \rrbracket = 0$ is inducing $k\#\mathcal{F}$ free constraints on a space of dimension $3kN$. This induces a space of dimension

$$3kN - k\#\mathcal{F} = 3kN - k \frac{3N}{2} = \frac{3kN}{2}.$$

Adding the dimension of theses different sets gives the dimension of $\ker \nabla_{\mathcal{D}'\cdot}$:

$$\begin{aligned} \dim(\ker \nabla_{\mathcal{D}'\cdot}) &= N \frac{k(k-1)}{2} + 1 + \frac{N}{2} + \frac{3kN}{2} \\ &= \frac{N}{2} (k^2 - k + 1 + 3k) + 1 \\ &= \frac{N(k+1)^2}{2} + 1, \end{aligned}$$

which is exactly equal to $\text{rank}(\nabla^\perp) + \dim \mathbb{K}$. We have then proven that $\text{Range}(\nabla^\perp) \oplus \mathbb{K} \subset \ker \nabla_{\mathcal{D}'\cdot}$ and that the dimensions are equal, so that $\text{Range}(\nabla^\perp) \oplus \mathbb{K} = \ker \nabla_{\mathcal{D}'\cdot}$. \square

4.5. Study of $\nabla_{\mathcal{D}'\cdot}$

The kernel of $\nabla_{\mathcal{D}'\cdot}$ was already characterised in Proposition 4.5. We now characterise its range.

PROPOSITION 4.6 (Range of $\nabla_{\mathcal{D}'\cdot}$). — *We have*

$$\text{d}\mathbb{P}_{k-1}(\mathcal{C}) \times \text{d}\mathbb{P}_k(\mathcal{F}) = \text{Range}(\nabla_{\mathcal{D}'\cdot}) \oplus \mathbb{K},$$

where the sum is orthogonal for the scalar product defined in (2.1).

Proof. — Following Proposition 4.5 and Proposition 4.2 we have

$$\dim(\ker \nabla_{\mathcal{D}'\cdot}) = \text{rank}(\nabla^\perp) + 2 = \frac{N(k+1)^2}{2} - 1 + 2 = \frac{N(k+1)^2}{2} + 1.$$

Using the rank nullity theorem gives

$$\dim(\text{d}\mathbb{P}_k) = \text{rank}(\nabla_{\mathcal{D}'\cdot}) + \dim(\ker \nabla_{\mathcal{D}'\cdot}).$$

Using Proposition 4.1 leads to

$$\begin{aligned}
 \text{rank}(\nabla_{\mathcal{D}'}) &= \dim \mathbf{dP}_k - \dim(\ker \nabla_{\mathcal{D}'}) \\
 &= N(k+1)(k+2) - \left(\frac{N(k+1)^2}{2} + 1 \right) \\
 &= \frac{N(k+1)(2(k+2) - (k+1))}{2} - 1 \\
 &= \frac{N(k+1)(2k+4-k-1)}{2} - 1 \\
 \text{rank}(\nabla_{\mathcal{D}'}) &= \frac{N(k+1)(k+3)}{2} - 1.
 \end{aligned}$$

We prove now that \mathbb{K} is orthogonal to $\text{Range}(\nabla_{\mathcal{D}'})$. We denote by k an element of $\mathbf{dP}_{k-1}(\mathcal{C}) \times \mathbf{dP}_k(\mathcal{F})$, which has the same value on all the cells and faces. We also denote by k this value. We denote by \mathbf{u} an element of $\mathbf{dP}_k(\mathcal{C})$. Then

$$\begin{aligned}
 \langle \nabla_{\mathcal{D}'} \cdot \mathbf{u} | k \rangle_{[\mathbf{dP}_{k-1}(\mathcal{C}) \times \mathbf{dP}_k(\mathcal{F})]} &= \sum_{c \in \mathcal{C}} \int_c k \nabla \cdot \mathbf{u} + \sum_{f \in \mathcal{F}} \int_f k [\mathbf{u} \cdot \mathbf{n}_f] \\
 &= \sum_{c \in \mathcal{C}} \int_c \nabla \cdot (k\mathbf{u}) + \sum_{f \in \mathcal{F}} \int_f k [\mathbf{u} \cdot \mathbf{n}_f] \\
 &= \sum_{c \in \mathcal{C}} \int_{\partial c} k\mathbf{u} \cdot \mathbf{n}_{out} + \sum_{f \in \mathcal{F}} \int_f k [\mathbf{u} \cdot \mathbf{n}_f] \\
 &= \sum_{c \in \mathcal{C}} \sum_{f \in \mathcal{F}(c)} \int_f k\mathbf{u} \cdot \mathbf{n}_{out} + \sum_{f \in \mathcal{F}} \int_f k [\mathbf{u} \cdot \mathbf{n}_f] \\
 &= \sum_{f \in \mathcal{F}} \int_f (k\mathbf{u}_L - k\mathbf{u}_R) \cdot \mathbf{n}_f + \sum_{f \in \mathcal{F}} \int_f k [\mathbf{u} \cdot \mathbf{n}_f] \\
 &= - \sum_{f \in \mathcal{F}} \int_f k [\mathbf{u} \cdot \mathbf{n}_f] + \sum_{f \in \mathcal{F}} \int_f k [\mathbf{u} \cdot \mathbf{n}_f] \\
 \langle \nabla_{\mathcal{D}'} \cdot \mathbf{u} | k \rangle_{[\mathbf{dP}_{k-1}(\mathcal{C}) \times \mathbf{dP}_k(\mathcal{F})]} &= 0.
 \end{aligned}$$

We thus have proven that $\text{Range}(\nabla_{\mathcal{D}'}) \perp \mathbb{K}$. As

$$\text{rank}(\nabla_{\mathcal{D}'}) = \dim(\mathbf{dP}_{k-1}(\mathcal{C}) \times \mathbf{dP}_k(\mathcal{F})) - 1,$$

this actually means that

$$\mathbf{dP}_{k-1}(\mathcal{C}) \times \mathbf{dP}_k(\mathcal{F}) = \text{Range}(\nabla_{\mathcal{D}'}) \oplus \mathbb{K},$$

which ends the proof. □

4.6. Summary on the de Rham complex

Gathering all the results of this section, the following proposition was proven

PROPOSITION 4.7. — *The discrete diagram*

$$\mathbb{P}_{k+1} \xrightarrow{\nabla^\perp} \mathbf{dP}_k(\mathcal{C}) \xrightarrow{\nabla_{\mathcal{D}'}} \mathbf{dP}_k(\mathcal{F}) \times \mathbf{dP}_{k-1}(\mathcal{C}),$$

where $\nabla_{\mathcal{D}'\cdot}$ is the $\nabla\cdot$ in the sense of distributions, ensures the Proposition 1.1. Moreover

$$\begin{cases} \mathbb{P}_{k+1}/\mathbb{K} = \ker(\nabla^\perp) \\ (\mathrm{d}\mathbb{P}_k(\mathcal{F}) \times \mathrm{d}\mathbb{P}_{k-1}(\mathcal{C})) / \mathbb{K} = \mathrm{Range}(\nabla_{\mathcal{D}'\cdot}). \end{cases}$$

By changing the representation of the linear forms, the following proposition is also obtained:

PROPOSITION 4.8. — *The discrete diagram*

$$\mathbb{P}_{k+1} \xrightarrow{\nabla} \mathbf{dP}_k(\mathcal{C}) \xrightarrow{\nabla_{\mathcal{D}'\cdot}^\perp} \mathrm{d}\mathbb{P}_k(\mathcal{F}) \times \mathrm{d}\mathbb{P}_{k-1}(\mathcal{C}),$$

where $\nabla_{\mathcal{D}'\cdot}^\perp$ is $\nabla^\perp\cdot$ in the sense of distributions, ensures the Proposition 1.1. Moreover

$$\begin{cases} \mathbb{P}_{k+1}/\mathbb{K} = \ker(\nabla) \\ (\mathrm{d}\mathbb{P}_k(\mathcal{F}) \times \mathrm{d}\mathbb{P}_{k-1}(\mathcal{C})) / \mathbb{K} = \mathrm{Range}(\nabla_{\mathcal{D}'\cdot}^\perp). \end{cases}$$

The location of the degrees of freedom for the two discrete de Rham complexes found for triangles are summarised in Figure 4.1. Note that compared with the finite element spaces $\mathbf{dRT}_{k+1}^\Delta$ and \mathbf{dN}_{k+1}^Δ discussed in Section 3, the space \mathbf{dP}_k represents a significant improvement regarding the number of degrees of freedom, as

$$\dim \mathbf{dRT}_{k+1}^\Delta - \mathbf{dP}_k = \mathbf{dN}_{k+1}^\Delta - \mathbf{dP}_k = k + 1.$$

Also, Raviart–Thomas and Nédélec finite element basis are known to be difficult to generate on simplices, whereas the generation of a basis for \mathbf{dP}_k is straightforward. Therefore, using the basis \mathbf{dP}_k instead of \mathbf{dRT}_{k+1} or \mathbf{dN}_{k+1} for discontinuous approximations seems to be very beneficial.

5. The case of Cartesian meshes

5.1. Why the Cartesian case is more complicated

Inspired by the \mathbf{dP}_0 triangular case, we consider the following discrete divergence

$$(5.1) \quad \begin{aligned} \nabla_{\mathcal{D}'\cdot} : \mathbf{dQ}_0 &\longmapsto \mathrm{d}\mathbb{P}_0(\mathcal{F}) \\ \mathbf{u} &\longmapsto a \text{ such that } a_f := \llbracket \mathbf{u} \cdot \mathbf{n}_f \rrbracket. \end{aligned}$$

We directly see that $\dim \mathbf{dQ}_0 = 2\#\mathcal{C} = 2N$ and $\dim \mathrm{d}\mathbb{P}_0(\mathcal{F}) = \#\mathcal{F} = 2N$. If N_x is the number of cells in the x direction and N_y is the number of cells in the y direction, then $N = N_x N_y$. Also, it is easy to see that $\ker \nabla_{\mathcal{D}'\cdot}$ is composed of $N_x + N_y$ components. This means that

$$\mathrm{rank} \nabla_{\mathcal{D}'\cdot} = 2N - N_x - N_y,$$

whereas we expect the $\nabla_{\mathcal{D}'\cdot}$ to be of rank $2N - 1$. Also, the kernel of the divergence is much smaller than what is expected for correctly approximating continuous divergence free vectors.

A second problem that we see is that when deriving an element of \mathbb{Q}_k , it does not give an element of \mathbb{Q}_{k-1} . Therefore, the finite element space that should be put

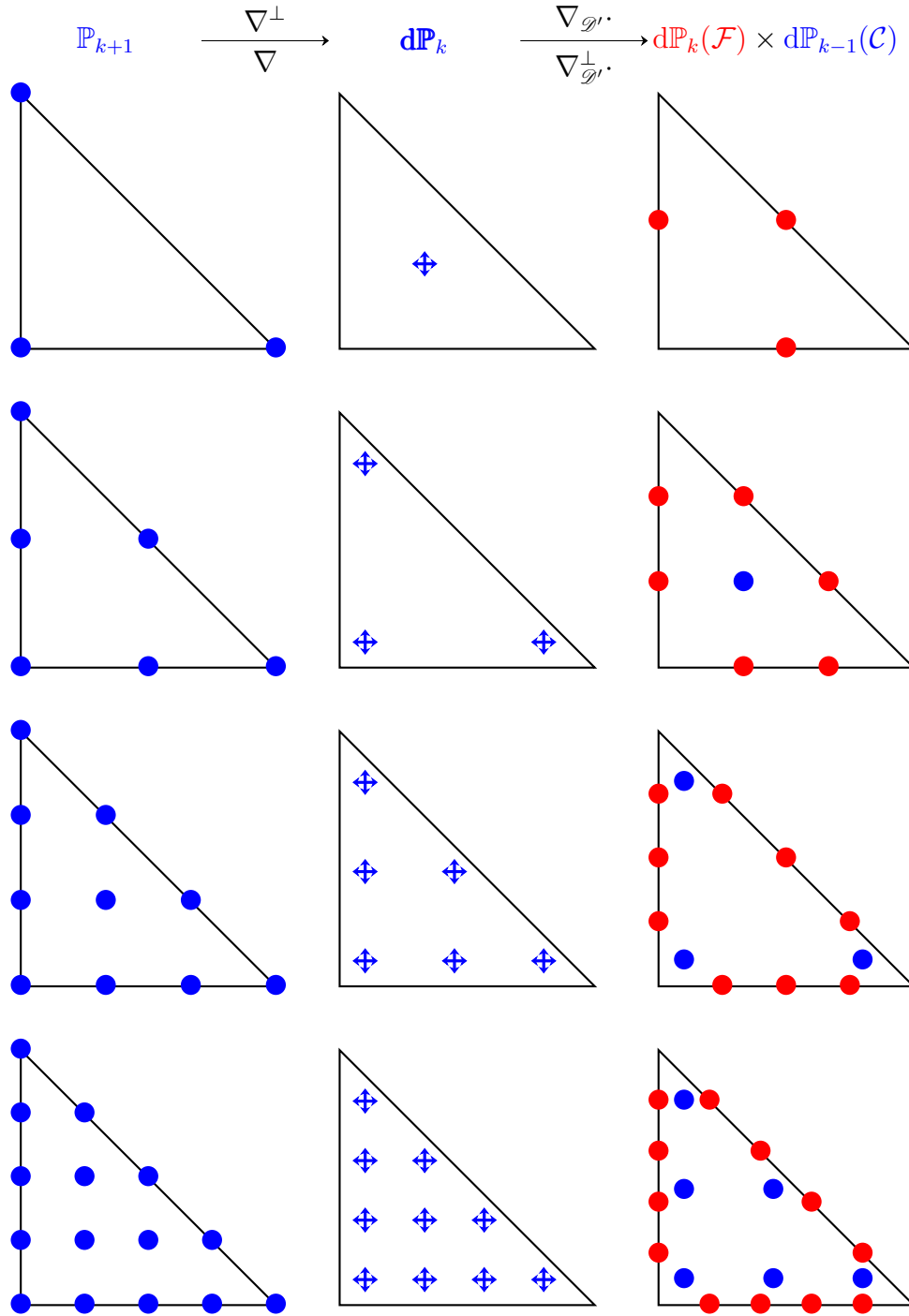


Figure 4.1. Representation of the finite element spaces involved in the grad/curl and curl/div de Rham complex for triangular meshes for $k = 0, 1, 2$ and 3 . Same code for colors are used as in Figure 3.1.

before the discrete ∇^\perp operator is difficult to determine. If we put \mathbb{Q}_0 , then the derivative will be 0 and the range of the discrete ∇^\perp will be reduced to 0. If \mathbb{Q}_1 is used, then the ∇^\perp will be in a space larger than \mathbb{Q}_0 .

5.2. Finite element space definition

We need to define some finite element spaces for discretising the different spaces, A , \mathbf{B} and C that are involved in the de Rham diagram (1.4). Based on what was done in the triangular case (4.1), we propose to start by the continuous finite element space \mathbb{Q}_{k+1} for the space A . For the space \mathbf{B} , the initial plan is to take $\mathbf{d}\mathbb{Q}_k$, but we need to enrich it with the curl of \mathbb{Q}_{k+1} . For simplifying, we relax the continuity conditions on $\nabla^\perp \mathbb{Q}_{k+1}$, and add to $\mathbf{d}\mathbb{Q}_k$ all the piecewise discontinuous polynomials that have the same degree as the one of $\nabla^\perp \mathbb{Q}_{k+1}$. This leads to choose $\widehat{\mathbf{d}\mathbb{Q}_k}^{\text{curl}}(\mathcal{C})$ for discretizing the space \mathbf{B} . Last, taking the divergence in the sense of distributions for $\widehat{\mathbf{d}\mathbb{Q}_k}^{\text{curl}}(\mathcal{C})$ naturally maps to $\mathbf{d}\mathbb{Q}_k(\mathcal{F}) \times \widehat{\mathbf{d}\mathbb{Q}_{k-1}}(\mathcal{C})$. This is why the following diagram is considered

$$(5.2) \quad \mathbb{Q}_{k+1} \xrightarrow{\nabla^\perp} \widehat{\mathbf{d}\mathbb{Q}_k}^{\text{curl}}(\mathcal{C}) \xrightarrow{\nabla_{\mathcal{F}} \cdot} \mathbf{d}\mathbb{Q}_k(\mathcal{F}) \times \widehat{\mathbf{d}\mathbb{Q}_{k-1}}(\mathcal{C}).$$

5.3. Dimension of the finite element spaces

We first compute the dimension of each of the finite element spaces involved in (5.2), induced by the number of faces, points and cells that was computed in Proposition 2.2.

PROPOSITION 5.1 (Dimension of the finite element spaces). —

$$\begin{cases} \dim \mathbb{Q}_{k+1} = N(k+1)^2 \\ \dim \widehat{\mathbf{d}\mathbb{Q}_k}^{\text{curl}}(\mathcal{C}) = N(2(k+1)^2 + 2k + 1) \\ \dim (\mathbf{d}\mathbb{Q}_k(\mathcal{F}) \times \widehat{\mathbf{d}\mathbb{Q}_{k-1}}(\mathcal{C})) = N(k^2 + 4k + 2) \end{cases}$$

Proof. — The dimension of \mathbb{Q}_{k+1} was already proven in Proposition 3.1. We are now interested in $\widehat{\mathbf{d}\mathbb{Q}_k}^{\text{curl}}(\mathcal{C})$. Let us recall that

$$\widehat{\mathbf{d}\mathbb{Q}_k}^{\text{curl}}(\mathcal{C}) = \left[(\mathbf{d}\mathbb{Q}_{k,k} + \mathbf{d}\mathbb{Q}_{k-1,k+1}) \times (\mathbf{d}\mathbb{Q}_{k,k} + \mathbf{d}\mathbb{Q}_{k+1,k-1}) \right] \oplus \text{Vec} \begin{pmatrix} x^k y^{k+1} \\ x^{k+1} y^k \end{pmatrix}.$$

We first focus on the dimension of $\mathbb{Q}_{k,k} + \mathbb{Q}_{k-1,k+1}$. The elements of $\mathbb{Q}_{k-1,k+1}$ are all in $\mathbb{Q}_{k,k}$, except for the case in which the degree in y is $k+1$. A basis of these polynomials that are in $\mathbb{Q}_{k-1,k+1}$ but not in $\mathbb{Q}_{k,k}$ is therefore given by $x^i y^{k+1}$ for $0 \leq i \leq k-1$, so that

$$\dim (\mathbb{Q}_{k,k} + \mathbb{Q}_{k-1,k+1}) = (k+1)^2 + k.$$

The space $\mathbb{Q}_{k,k} + \mathbb{Q}_{k+1,k-1}$ has the same dimension, so that

$$\begin{aligned} \dim \widehat{\mathbf{d}\mathbb{Q}}_k^{\text{curl}}(\mathcal{C}) &= N \left(\dim(\mathbb{Q}_{k,k} + \mathbb{Q}_{k-1,k+1}) + \dim(\mathbb{Q}_{k,k} + \mathbb{Q}_{k+1,k-1}) + 1 \right) \\ &= N \left(2 \left((k+1)^2 + k \right) + 1 \right) \\ \dim \widehat{\mathbf{d}\mathbb{Q}}_k^{\text{curl}}(\mathcal{C}) &= N \left(2(k+1)^2 + 2k + 1 \right). \end{aligned}$$

It remains to compute the dimension of $\mathbf{d}\mathbb{Q}_k(\mathcal{F}) \times \widehat{\mathbf{d}\mathbb{Q}}_{k-1}(\mathcal{C})$. We recall that

$$\widehat{\mathbf{d}\mathbb{Q}}_{k-1}(\mathcal{C}) = \mathbf{d}\mathbb{Q}_{k-1}(\mathcal{C}) + \mathbf{d}\mathbb{Q}_{k,k-1}(\mathcal{C}) + \mathbf{d}\mathbb{Q}_{k-1,k}(\mathcal{C}).$$

This leads to

$$\begin{aligned} \dim \widehat{\mathbf{d}\mathbb{Q}}_{k-1}(\mathcal{C}) &= N \left(k^2 + 2k \right) \\ &= Nk(k+2). \end{aligned}$$

We finally find

$$\begin{aligned} \dim \left(\mathbf{d}\mathbb{Q}_k(\mathcal{F}) \times \widehat{\mathbf{d}\mathbb{Q}}_{k-1}(\mathcal{C}) \right) &= \dim(\mathbf{d}\mathbb{Q}_k(\mathcal{F})) + \dim \widehat{\mathbf{d}\mathbb{Q}}_{k-1}(\mathcal{C}) \\ &= \#\mathcal{F}(k+1) + Nk(k+2) \\ &= 2N(k+1) + Nk(k+2) \\ \dim \left(\mathbf{d}\mathbb{Q}_k(\mathcal{F}) \times \widehat{\mathbf{d}\mathbb{Q}}_{k-1}(\mathcal{C}) \right) &= N \left(k^2 + 4k + 2 \right). \end{aligned} \quad \square$$

5.4. Study of $\nabla_{\mathcal{D}'}^\perp$

We are now interested in the study of the $\nabla_{\mathcal{D}'}^\perp$ operator.

PROPOSITION 5.2 ($\nabla_{\mathcal{D}'}^\perp$ in the quadrangular case). — We have

$$\begin{cases} \dim(\ker \nabla_{\mathcal{D}'}^\perp) = 1 \\ \text{rank}(\nabla_{\mathcal{D}'}^\perp) = N(k+1)^2 - 1. \end{cases}$$

The proof is exactly the same as Proposition 4.2.

5.5. Discrete divergence free polynomials on the reference cell

We consider the following application

$$(5.3) \quad \mathbf{C}_k^\partial : \psi \in \mathbf{d}\mathbb{Q}_{k+1}(\widehat{K}) \longmapsto \mathbf{Tr}(\nabla^\perp \psi) \in \mathbf{d}\mathbb{P}_k(\partial \widehat{K})$$

PROPOSITION 5.3. — We denote by \mathbb{k} the constant elements of $\mathbf{d}\mathbb{P}_k(\partial \widehat{K})$. Then

$$\mathbf{d}\mathbb{P}_k(\partial \widehat{K}) = \text{Range } \mathbf{C}_k^\partial \oplus \mathbb{k},$$

where the sum is orthogonal.

Proof. — The proof that the sum of $\text{Range } \mathbf{C}_k^\partial$ and \mathbb{k} is direct and orthogonal follows exactly the same lines as the proof for the triangular case of Proposition 4.3.

We are now interested in the study of the kernel of \mathbf{C}_k^∂ . Suppose that an element ψ is such that $\mathbf{C}_k^\partial(\psi) = 0$. We consider the classical Lagrange basis of $\text{d}\mathbb{Q}_{k+1}(\widehat{K})$. Then ψ is such that its value on the boundary of \widehat{K} is constant, and may take any value on the degrees of freedom matching with the interior nodes. This means that

$$\dim(\ker \mathbf{C}_k^\partial) = 1 + k^2.$$

Using the rank-nullity theorem gives

$$\begin{aligned} \text{rank}(\mathbf{C}_k^\partial) &= \dim \text{d}\mathbb{Q}_{k+1} - (1 + k^2) \\ &= (k+2)^2 - 1 - k^2 \\ &= k^2 + 4k + 4 - 1 - k^2 \\ \text{rank}(\mathbf{C}_k^\partial) &= 4k + 3. \end{aligned}$$

We also know that $\dim \text{d}\mathbb{P}_k(\partial\widehat{K}) = 4(k+1)$. We have then $\text{Range } \mathbf{C}_k^\partial \oplus \mathbb{k} \subset \text{d}\mathbb{P}_k(\partial\widehat{K})$, and $\dim(\text{Range } \mathbf{C}_k^\partial \oplus \mathbb{k}) = \dim \text{d}\mathbb{P}_k(\partial\widehat{K})$, so that $\text{Range } \mathbf{C}_k^\partial \oplus \mathbb{k} = \text{d}\mathbb{P}_k(\partial\widehat{K})$, which ends the proof. \square

PROPOSITION 5.4 (Decomposition of divergence free elements). — We denote by $\mathcal{L}^{f,i}$ the Legendre polynomial of degree i on the face f of \widehat{K} , normalised such that

$$\int_{\partial\widehat{K}} (\mathcal{L}^{f,i})^2 = 1.$$

Suppose that $\mathbf{u} \in \widehat{\text{d}\mathbb{Q}_k^{\text{curl}}}(\widehat{K})$ is divergence free. Then \mathbf{u} can be uniquely decomposed as

$$\mathbf{u} = \bar{\mathbf{v}}_{\mathbf{u}}^0 + \bar{\mathbf{v}}_{\mathbf{u}}^1 + \sum_{f \in \mathcal{F}(\widehat{K})} \sum_{i=1}^k \bar{\mathbf{v}}_{\mathbf{u}}^{f,i},$$

where

- $\bar{\mathbf{v}}_{\mathbf{u}}^0$ is in the set

$$\Phi_k = \left\{ \mathbf{u} \in \widehat{\text{d}\mathbb{Q}_k^{\text{curl}}} \mid \nabla \cdot \mathbf{u} = 0 \quad \text{Tr}(\mathbf{u}) = 0 \right\}.$$

- $\bar{\mathbf{v}}_{\mathbf{u}}^1$ is in $\text{Vec}((\frac{1}{0}), (\frac{0}{1}), (\frac{1-2x}{2y-1}))$.
- $\bar{\mathbf{v}}_{\mathbf{u}}^{f,i}$ is orthogonal to Φ_k and such that
 - $\nabla \cdot \bar{\mathbf{v}}_{\mathbf{u}}^{f,i} = 0$.
 - $\text{Tr}(\bar{\mathbf{v}}_{\mathbf{u}}^{f,i})$ is orthogonal to all $\mathcal{L}^{g,j}$ for $\{g,j\} \neq \{f,i\}$.

Proof. — We first prove that $\bar{\mathbf{v}}_{\mathbf{u}}^1 \perp \Phi_k$. We denote by \mathbf{u}_Φ an element of Φ_k . As in the proof of Proposition 4.4, a ψ^Φ exists such that $\mathbf{u}_\Phi = \nabla^\perp \Psi^\Phi$, and the trace of Ψ^Φ

is constant. Then

$$\begin{aligned}
\int_{\hat{K}} \bar{\mathbf{v}}_{\mathbf{u}}^1 \cdot \mathbf{u}_{\Phi} &= \int_{\hat{K}} \bar{\mathbf{v}}_{\mathbf{u}}^1 \cdot \nabla^{\perp} \Psi^{\Phi} \\
&= \int_{\hat{K}} \left(\bar{\mathbf{v}}_{\mathbf{u}}^1 \right)^{\perp} \cdot \nabla \Psi^{\Phi} \\
&= \int_{\hat{K}} \nabla \cdot \left(\left(\bar{\mathbf{v}}_{\mathbf{u}}^1 \right)^{\perp} \Psi^{\Phi} \right) - \int_{\hat{K}} \nabla \cdot \left(\left(\bar{\mathbf{v}}_{\mathbf{u}}^1 \right)^{\perp} \right) \Psi^{\Phi} \\
&= \int_{\partial \hat{K}} \mathbf{Tr} \left(\left(\bar{\mathbf{v}}_{\mathbf{u}}^1 \right)^{\perp} \Psi^{\Phi} \right) \\
\int_{\hat{K}} \bar{\mathbf{v}}_{\mathbf{u}}^1 \cdot \mathbf{u}_{\Phi} &= \text{Tr} \left(\Psi^{\Phi} \right) \int_{\partial \hat{K}} \mathbf{Tr} \left(\left(\bar{\mathbf{v}}_{\mathbf{u}}^1 \right)^{\perp} \right),
\end{aligned}$$

because $\nabla \cdot \left(\left(\bar{\mathbf{v}}_{\mathbf{u}}^1 \right)^{\perp} \right) = 0$, and because $\text{Tr}(\Psi^{\Phi})$ is constant. Computing the integral on $\partial \hat{K}$ of all the components of $\left(\bar{\mathbf{v}}_{\mathbf{u}}^1 \right)^{\perp}$ (namely $(1, 0)^T$, $(0, 1)^T$ and $(1 - 2x, 2y - 1)^T$) leads to

$$\int_{\hat{K}} \bar{\mathbf{v}}_{\mathbf{u}}^1 \cdot \mathbf{u}_{\Phi} = 0.$$

We have then proven that $\bar{\mathbf{v}}_{\mathbf{u}}^1 \perp \Phi_k$. The proof of uniqueness follows exactly the same lines as the proof of Proposition 4.4.

The strategy for the existence begins similarly but then differs. We consider one $\mathcal{L}^{f,i}$ of $d\mathbb{P}_k(\partial \hat{K})$, for $i \geq 1$. Then, as was done in the proof of Proposition 4.4, a $\psi^{f,i}$ exists such that $\mathbf{C}_k^{\partial}(\psi^{f,i}) = \mathcal{L}^{f,i}$. Denoting by \mathcal{P} the orthogonal projection on Φ_k , we define $\mathbf{e}^{f,i} := \nabla^{\perp}(\psi^{f,i}) - \mathcal{P}(\nabla^{\perp}(\psi^{f,i}))$. Then $\mathbf{e}^{f,i}$ is orthogonal to Φ_k , is divergence free, and is such that $\mathbf{Tr}(\mathbf{e}^{f,i}) = \mathcal{L}^{f,i}$. We consider now one divergence free $\mathbf{u} \in \widehat{\mathbf{dQ}}_k^{\text{curl}}(\hat{K})$. We define

$$\lambda_{f,i} := \int_{\partial \hat{K}} \mathbf{Tr}(\mathbf{u}) \mathcal{L}^{f,i},$$

and set $\bar{\mathbf{v}}_{\mathbf{u}}^{f,i} = \lambda_{f,i} \mathbf{e}^{f,i}$. We also set $\bar{\mathbf{v}}_{\mathbf{u}}^0 = \mathcal{P}(\mathbf{u})$, and

$$\bar{\mathbf{v}}_{\mathbf{u}}^1 := \mathbf{u} - \bar{\mathbf{v}}_{\mathbf{u}}^0 - \sum_{f \in \mathcal{F}(\hat{K})} \sum_{i=1}^k \bar{\mathbf{v}}_{\mathbf{u}}^{f,i}.$$

Then $\bar{\mathbf{v}}_{\mathbf{u}}^0$ and the $\bar{\mathbf{v}}_{\mathbf{u}}^{f,i}$ ensure all the properties required. It remains to prove that $\bar{\mathbf{v}}_{\mathbf{u}}^1$ is in the expected space. We know that $\bar{\mathbf{v}}_{\mathbf{u}}^1$ is divergence free, orthogonal to Φ_k , and that its trace is constant on each face, because all the components in $\mathcal{L}^{f,i}$ for $i \geq 1$ were removed. We denote by b_0, b_1, b_2 and b_3 the values of the trace on the boundary of $\bar{\mathbf{v}}_{\mathbf{u}}^1$ (see Figure 5.1).

We then define

$$\mathbf{k} := \frac{b_1 - b_3}{2} \begin{pmatrix} 1 \\ 0 \end{pmatrix} + \frac{b_2 - b_0}{2} \begin{pmatrix} 0 \\ 1 \end{pmatrix} + \frac{b_0 + b_2}{2} \begin{pmatrix} 1 - 2x \\ 2y - 1 \end{pmatrix},$$

then $\text{Tr}(\mathbf{k}) = \text{Tr}(\bar{\mathbf{v}}_{\mathbf{u}}^1)$ (note that as $\nabla \cdot \bar{\mathbf{v}}_{\mathbf{u}}^1 = 0$, we have $b_0 + b_1 + b_2 + b_3 = 0$). Also, \mathbf{k} is divergence free and orthogonal to Φ_k . This means that $\bar{\mathbf{v}}_{\mathbf{u}}^1 - \mathbf{k}$ is divergence free and orthogonal to Φ_k . But as $\text{Tr}(\bar{\mathbf{v}}_{\mathbf{u}}^1 - \mathbf{k}) = 0$, $\bar{\mathbf{v}}_{\mathbf{u}}^1 - \mathbf{k}$ is also in Φ_k , and so $\bar{\mathbf{v}}_{\mathbf{u}}^1 - \mathbf{k} = 0$, which proves that $\bar{\mathbf{v}}_{\mathbf{u}}^1$ is in $\text{Vec}((\begin{smallmatrix} 1 \\ 0 \end{smallmatrix}), (\begin{smallmatrix} 0 \\ 1 \end{smallmatrix}), (\begin{smallmatrix} 1-2x \\ 2y-1 \end{smallmatrix}))$. This ends the proof of Proposition 5.4. \square

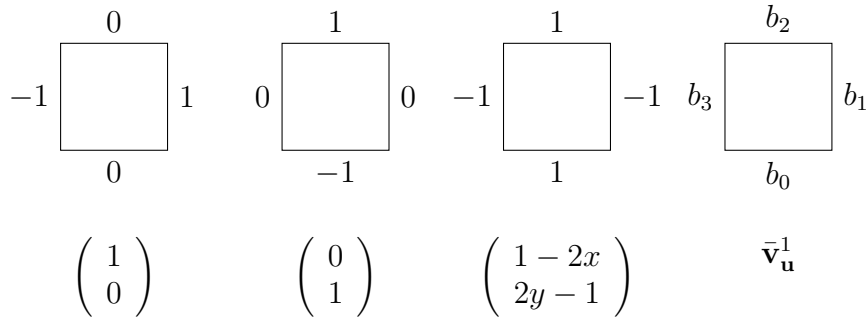


Figure 5.1. Value of the trace for $\bar{\mathbf{v}}_{\mathbf{u}}^1$ and the basis used for representing it.

It is important to note that the decomposition of Proposition 5.4 was proven on the reference element, but holds also on all the cells of a Cartesian meshes, the basis function $\begin{pmatrix} 1-2x \\ 2y-1 \end{pmatrix}$ being replaced by $\begin{pmatrix} \frac{2}{L_x}(m_x-x) \\ \frac{2}{L_y}(y-m_y) \end{pmatrix}$, where (m_x, m_y) is the centre of the cell and L_x and L_y are the size of the cell in the directions x , and y .

5.6. $\ker(\nabla_{\mathcal{D}'})$ and $\text{Range}(\nabla^\perp)$

PROPOSITION 5.5. — We denote by \mathbb{K} the set of uniform vectors. Then

$$\ker(\nabla_{\mathcal{D}'}) = \text{Range}(\nabla^\perp) \oplus \mathbb{K}.$$

Proof. — The proof of $\text{Range}(\nabla^\perp)$ and \mathbb{K} being orthogonal and the two being subvectorial spaces of $\ker(\nabla_{\mathcal{D}'})$ is exactly the same as in the proof of Proposition 4.5.

Concerning the dimension of this space, we proceed as in the proof of Proposition 4.5, but need to rewrite it because the dimensions are different. Suppose now that an element $\mathbf{u} \in \widehat{\mathbf{dQ}}_k^{\text{curl}}$ is such that its divergence $\nabla_{\mathcal{D}'}$ is 0, namely

$$\begin{cases} \forall c \in \mathcal{C} & \nabla \cdot \mathbf{u} = 0 \\ \forall f \in \mathcal{F} & \llbracket \mathbf{u} \cdot \mathbf{n}_f \rrbracket = 0. \end{cases}$$

As $\nabla \cdot \mathbf{u} = 0$ on all the cells, \mathbf{u} can be decomposed as in Proposition 5.4; this decomposition involves three types of components:

- The ones of Φ_k , which have a trace equal to 0. This set is of dimension $k^2 + 1$ on each cell.
- One component in the dimension 3 vectorial space.

$$\widehat{\mathbb{K}} = \text{Vec} \left(\begin{pmatrix} 1 \\ 0 \end{pmatrix}, \begin{pmatrix} 0 \\ 1 \end{pmatrix}, \begin{pmatrix} \frac{2}{L_{i,j}^x} (m_{i,j}^x - x) \\ \frac{2}{L_{i,j}^y} (y - m_{i,j}^y) \end{pmatrix} \right).$$

- The components $\bar{\mathbf{v}}_i^f$ for $1 \leq i \leq k$ and for all faces. This set is of dimension $4k$ on each cell.

Let us see now what is the effect of the constraint $\llbracket \mathbf{u} \cdot \mathbf{n}_f \rrbracket = 0$ on these different components. We first remark that the traces of the different components are orthogonal two at a time, which means that we can consider the effect of $\llbracket \mathbf{u} \cdot \mathbf{n}_f \rrbracket = 0$ component by component:

- The ones of Φ_k are not affected by the zero jump constraint, because their trace is already equal to 0. This induces $N k^2$ components in $\widehat{\mathbf{dQ}}_k^{\text{curl}}$.
- The components of $\widehat{\mathbf{K}}$, with the constraint $\llbracket \mathbf{u} \cdot \mathbf{n}_f \rrbracket = 0$ is a set that is identified in Proposition A.1, proven in Appendix A: it is of dimension $N + 1$.
- Concerning the components $\bar{\mathbf{v}}_i^f$ for $1 \leq i \leq k$, the constraint $\llbracket \mathbf{u} \cdot \mathbf{n}_f \rrbracket = 0$ is inducing $k\#\mathcal{F}$ free constraints on a space of dimension $4kN$. This induces a space of dimension

$$4kN - k\#\mathcal{F} = 4kN - k2N = 2kN.$$

Adding the dimension of these different sets gives the dimension of $\ker \nabla_{\mathcal{G}'}$:

$$\begin{aligned} \dim(\ker \nabla_{\mathcal{G}'}) &= Nk^2 + N + 1 + 2kN \\ &= N(k^2 + 2k + 1) + 1 \\ &= N(k + 1)^2 + 1, \end{aligned}$$

which is exactly equal to $\text{rank}(\nabla^\perp) + \dim \mathbf{K}$. We have then proven that $\nabla^\perp \oplus \mathbf{K} \subset \ker \nabla_{\mathcal{G}'}$ and that the dimensions are equal, so that $\text{Range}(\nabla^\perp) \oplus \mathbf{K} = \ker \nabla_{\mathcal{G}'}$. \square

5.7. Study of $\nabla_{\mathcal{G}'}$.

The kernel of $\nabla_{\mathcal{G}'}$ was already characterised in Proposition 5.5. We now characterise its range.

PROPOSITION 5.6 (Range of $\nabla_{\mathcal{G}'}$). — *We have*

$$\widehat{\mathbf{dQ}}_{k-1}(\mathcal{C}) \times \mathbf{dQ}_k(\mathcal{F}) = \text{Range}(\nabla_{\mathcal{G}'}) \oplus \mathbf{K},$$

where the sum is orthogonal for the scalar product defined in (2.1).

The proof is exactly the same as the proof of Proposition 4.6.

5.8. Summary on the de Rham complex

Gathering all the results of this section, the following proposition was proven

PROPOSITION 5.7. — *The discrete diagram*

$$\mathbb{P}_{k+1} \xrightarrow{\nabla^\perp} \widehat{\mathbf{dQ}}_k^{\text{curl}}(\mathcal{C}) \xrightarrow{\nabla_{\mathcal{G}'}} \mathbf{dQ}_k(\mathcal{F}) \times \widehat{\mathbf{dQ}}_{k-1}(\mathcal{C}),$$

where $\nabla_{\mathcal{G}'}$ is $\nabla \cdot$ in the sense of distributions, ensures the Proposition 1.1. Moreover

$$\begin{cases} \mathbb{Q}_{k+1}/\mathbb{K} = \ker(\nabla_{\mathcal{G}'}^\perp) \\ \left(\mathbf{dQ}_k(\mathcal{F}) \times \widehat{\mathbf{dQ}}_{k-1}(\mathcal{C}) \right) / \mathbb{K} = \text{Range}(\nabla_{\mathcal{G}'}). \end{cases}$$

By changing the representation of the linear forms, which is equivalent to rotating of $\pi/2$ the vector spaces, the following proposition is also obtained:

PROPOSITION 5.8. — *The discrete diagram*

$$\mathbb{Q}_{k+1} \xrightarrow{\nabla} \widehat{\mathbf{dQ}}_k^{\text{div}}(\mathcal{C}) \xrightarrow{\nabla_{\mathcal{D}'}^\perp} \mathbf{dQ}_k(\mathcal{F}) \times \widehat{\mathbf{dQ}}_{k-1}(\mathcal{C}),$$

where $\nabla_{\mathcal{D}'}^\perp \cdot$ is $\nabla^\perp \cdot$ in the sense of distributions, ensures the Proposition 1.1. Moreover

$$\begin{cases} \mathbb{Q}_{k+1}/\mathbb{K} = \ker(\nabla) \\ (\mathbf{dQ}_k(\mathcal{F}) \times \widehat{\mathbf{dQ}}_{k-1}(\mathcal{C}))/\mathbb{K} = \text{Range}(\nabla_{\mathcal{D}'}^\perp \cdot). \end{cases}$$

We now compare the number of degrees of freedom of the basis $\widehat{\mathbf{dQ}}_k^{\text{div}}$ and $\widehat{\mathbf{dQ}}_k^{\text{curl}}$ with the quadrangular basis discussed in Section 3 on each cell:

$$\begin{aligned} \dim \widehat{\mathbf{dQ}}_k^{\text{div}} - \dim \mathbf{dRT}_{k+1}^\square &= \dim \widehat{\mathbf{dQ}}_k^{\text{curl}} - \dim \mathbf{dN}_{k+1}^\square \\ &= 2(k+2)(k+1) - (2(k+1)^2 + 2k+1) \\ &= 1. \end{aligned}$$

Therefore the difference of number of degrees of freedom is negligible. Considering that the vector basis $\widehat{\mathbf{dQ}}_k^{\text{div}}$ and $\widehat{\mathbf{dQ}}_k^{\text{curl}}$ do not have a Lagrange basis (this is why no representation of these basis was proposed), it seems that using these new basis has few benefits with respect to \mathbf{dRT}_{k+1} and \mathbf{dN}_{k+1} .

6. Conclusion

In this article, two-dimensional discrete de Rham structures in which the vector space is a discontinuous approximation space were discussed. We first recalled that by relaxing the normal or tangential continuity properties of the classical conformal space, a set of discontinuous approximation space can be designed as in [Lic17]. These discontinuous spaces, \mathbf{dN} and \mathbf{dRT} , are discontinuous versions of the Nédélec \mathbf{N} and Raviart–Thomas \mathbf{RT} approximation spaces.

Then the de Rham structure of the natural discontinuous vectorial space \mathbf{dP}_k on triangles, used for example for the discontinuous Galerkin method was investigated. We proved that for straight triangular meshes, a discrete de Rham complex can be built for which the Proposition 1.1 is ensured for any order of approximation.

Based on the finite element spaces and discrete $\nabla^\perp/(\nabla_{\mathcal{D}'}^\perp \cdot)$ or $\nabla/(\nabla_{\mathcal{D}'}^\perp \cdot)$ that were used for the triangular case, Proposition 1.1 was proven for discontinuous spaces of vectors. However, the space of vectors is not the classical \mathbf{dQ}_k approximation space which is usually used in the discontinuous Galerkin method, but rather an enriched version, $\widehat{\mathbf{dQ}}_k^{\text{curl}}$ and $\widehat{\mathbf{dQ}}_k^{\text{div}}$, depending on the diagram considered. Note that no diagram that would be based on the so-called serendipity elements was addressed, but this could be a way to derive velocity approximation spaces that can be put in a de Rham diagram with fewer degrees of freedom (still at the price of getting a nonoptimal order of accuracy on general quads).

It is important to note that only Proposition 1.1 was addressed in this article. The bounded cochain projection property was not addressed, which is still far from the framework that was developed in [Arn18] for conforming finite element approximation. Still, Proposition 1.1 is an algebraic property that we believe to be useful in the context of the derivation of curl preserving numerical schemes for hyperbolic systems. Some curl-preserving schemes that were developed in the finite volume scheme context [DJOR16, DOR10, JP22] rely on the existence of the following discrete decomposition [AF89] (\mathbb{CR} denotes the Crouzeix–Raviart finite element space [CR74]), which reads on periodic triangular meshes as

$$(6.1) \quad \mathbf{dP}_0/\mathbb{R}^2 = \nabla^\perp \mathbb{P}_1 \oplus \nabla \mathbb{CR},$$

and on the preservation of the solenoidal component, this property being strongly linked with the correct low Mach number behaviour on triangular and tetrahedral meshes [Gui09, JP24a]. The Proposition 1.1 discussed in this article directly induces the following Hodge–Helmholtz decomposition [Arn18]:

$$(6.2) \quad \mathbf{B}/\mathbb{R}^2 = \text{Range}(\nabla^\perp) \oplus \text{Range}(\nabla_{\mathcal{D}'\star}),$$

where the \star denotes the adjoint operator. For example, the diagram of Proposition 4.7 induces the following discrete Hodge–Helmholtz decomposition

$$(6.3) \quad \mathbf{dP}_k(\mathcal{C})/\mathbb{R}^2 = \text{Range}(\nabla^\perp \mathbb{P}_{k+1}) \oplus \text{Range}(\nabla_{\mathcal{D}'\star}(\mathbf{dP}_k(\mathcal{F}) \times \mathbf{dP}_{k-1}(\mathcal{C}))),$$

which can be seen as the high order extension of (6.1). In a submitted article [Per24], we explain how to preserve a curl or a divergence constraint of a hyperbolic system of conservation law with the approximation spaces that were discussed in this article.

Appendix A. Proof for low order quads

PROPOSITION A.1. — *Suppose that a periodic Cartesian mesh is composed of N cells, and that on each cell (of mid point $(m_{i,j}^x, m_{i,j}^y)$ and of length $L_{i,j}^x$ and $L_{i,j}^y$), a vector \mathbf{u} is in*

$$\text{Vec} \left(\begin{pmatrix} 1 \\ 0 \end{pmatrix}, \begin{pmatrix} 0 \\ 1 \end{pmatrix}, \begin{pmatrix} \frac{2}{L_{i,j}^x} (m_{i,j}^x - x) \\ \frac{2}{L_{i,j}^y} (y - m_{i,j}^y) \end{pmatrix} \right),$$

then the vectorial space such that

$$(A.1) \quad \forall f \quad \llbracket \mathbf{u} \cdot \mathbf{n}_f \rrbracket = 0,$$

is of dimension $N + 1$.

Proof. — We denote by N_x (resp. N_y) the number of cells in the x (resp. y) direction. For each cell i, j , we denote by $\alpha_{i,j}$, $\beta_{i,j}$ and $\gamma_{i,j}$ the coefficients such that

$$\mathbf{u}_{|c_{i,j}} = \alpha_{i,j} \begin{pmatrix} 1 \\ 0 \end{pmatrix} + \beta_{i,j} \begin{pmatrix} 0 \\ 1 \end{pmatrix} + \gamma_{i,j} \begin{pmatrix} \frac{2}{L_{i,j}^x} (m_{i,j}^x - x) \\ \frac{2}{L_{i,j}^y} (y - m_{i,j}^y) \end{pmatrix}.$$

Then the constraint $\llbracket \mathbf{u} \cdot \mathbf{n}_f \rrbracket = 0$ is equivalent to the following equations

$$(A.2) \quad \forall j \quad \begin{cases} \forall 0 \leq i \leq N_x - 2 & \alpha_{i+1,j} - \alpha_{i,j} = -(\gamma_{i+1,j} + \gamma_{i,j}) \\ \alpha_{0,j} - \alpha_{N_x-1,j} = -(\gamma_{0,j} + \gamma_{N_x-1,j}) \end{cases}$$

$$(A.3) \quad \forall i \quad \begin{cases} \forall 0 \leq j \leq N_y - 2 & \beta_{i,j+1} - \beta_{i,j} = -(\gamma_{i,j+1} + \gamma_{i,j}) \\ \beta_{i,0} - \beta_{i,N_y-1} = -(\gamma_{i,0} + \gamma_{i,N_y-1}) \end{cases}$$

We first consider equation (A.2). If this equation is seen for each j as a system in $\alpha_{\star,j}$, then this system is singular, with a kernel directed by $(1, 1, \dots, 1)$, and the right hand side is compatible with this kernel if and only if

$$(A.4) \quad \forall j \quad \sum_i \gamma_{i,j} = 0.$$

If this last constraint holds, then if one $\alpha_{\star,j}$ is known (for example $\alpha_{0,j}$), then the $\alpha_{i,j}$ are known for all i . This makes N_y parameters for recovering the $\alpha_{i,j}$ once the $\gamma_{i,j}$ are known.

In the same manner, by considering (A.3), we can prove that if and only if

$$(A.5) \quad \forall i \quad \sum_j \gamma_{i,j} = 0,$$

the system in β has a N_x parameter family solution determined by the $\beta_{i,0}$.

It remains to study the system on the γ coefficients defined by (A.4),(A.5). For this system, we consider the coefficients $\gamma_{i,j}$ for $i > 0$ and for $j > 0$ as parameters (this makes $N - (N_x + N_y - 1) = N - N_x - N_y + 1$ parameters). Then the $\gamma_{0,j}$ for $j \geq 1$ are determined by (A.4), and the $\gamma_{i,0}$ for $i \geq 1$ are determined by (A.5):

$$(A.6) \quad \begin{aligned} \forall j \geq 1 \quad \gamma_{0,j} &= - \sum_{i \geq 1} \gamma_{i,j} \\ \forall i \geq 1 \quad \gamma_{i,0} &= - \sum_{j \geq 1} \gamma_{i,j} \end{aligned}$$

It remains to determine $\gamma_{0,0}$, which is a priori given by two equations

$$\begin{aligned} \gamma_{0,0} &= - \sum_{i \geq 1} \gamma_{i,0} \\ \gamma_{0,0} &= - \sum_{j \geq 1} \gamma_{0,j} \end{aligned}$$

However, if (A.6) is considered, the two equations give the same value, namely

$$\gamma_{0,0} = - \sum_{i \geq 1} \sum_{j \geq 1} \gamma_{i,j}.$$

We therefore have been able to express all the $\gamma_{0,j}$ and all the $\gamma_{i,0}$ provided all the $\gamma_{i,j}$ for $i \geq 1$ and $j \geq 1$ are known.

Finally, a basis of the vectorial space determined by (A.1) was found. Its parameters are

- the $\gamma_{i,j}$ for $i \geq 1$ and $j \geq 1$. These are $N - N_x - N_y + 1$ parameters.

- The $\alpha_{0,j}$ for $j \geq 0$. These are N_y parameters.
- The $\beta_{i,0}$ for $i \geq 0$. These are N_x parameters.

This makes a total of $N + 1$ parameters. □

BIBLIOGRAPHY

- [ABF05] Douglas N. Arnold, Daniele Boffi, and Richard S. Falk, *Quadrilateral $H(\text{div})$ finite elements*, SIAM J. Numer. Anal. **42** (2005), no. 6, 2429–2451. ↑423
- [AF89] Douglas N. Arnold and Richard S. Falk, *A uniformly accurate finite element method for the Reissner-Mindlin plate*, SIAM J. Numer. Anal. **26** (1989), 1276–1290. ↑437, 448
- [AFW06] Douglas N. Arnold, Richard S. Falk, and Ragnar Winther, *Finite element exterior calculus, homological techniques, and applications*, Acta Numer. **15** (2006), 1–155. ↑420
- [AFW10] ———, *Finite element exterior calculus: from Hodge theory to numerical stability*, Bull. Am. Math. Soc. **47** (2010), no. 2, 281–354. ↑420
- [AL14] Douglas N. Arnold and Anders B. Logg, *Periodic table of the finite elements*, SIAM News **47** (2014), no. 9. ↑419, 423, 434
- [Arn18] Douglas N. Arnold, *Finite element exterior calculus*, CBMS-NSF Regional Conference Series in Applied Mathematics, vol. 93, Society for Industrial and Applied Mathematics, 2018. ↑420, 421, 448
- [Bal01] Dinshaw S. Balsara, *Divergence-free adaptive mesh refinement for magnetohydrodynamics*, J. Comput. Phys. **174** (2001), no. 2, 614–648. ↑421
- [Bal04] ———, *Second-order-accurate schemes for magnetohydrodynamics with divergence-free reconstruction*, Astrophys. J., Suppl. Ser. **151** (2004), no. 1, 149–184. ↑421
- [BDM85] Franco Brezzi, Jim Douglas, and Luisa D. Marini, *Two families of mixed finite elements for second order elliptic problems*, Numer. Math. **47** (1985), no. 2, 217–235. ↑434
- [BE14] Jérôme Bonelle and Alexandre Ern, *Analysis of compatible discrete operator schemes for elliptic problems on polyhedral meshes*, ESAIM, Math. Model. Numer. Anal. **48** (2014), no. 2, 553–581. ↑420
- [BE15] ———, *Analysis of compatible discrete operator schemes for the Stokes equations on polyhedral meshes*, IMA J. Numer. Anal. **35** (2015), no. 4, 1672–1697. ↑420
- [BF91] Franco Brezzi and Michel Fortin, *Mixed and hybrid finite element methods*, Springer Series in Computational Mathematics, vol. 15, Springer, 1991. ↑433
- [Bon14] Jérôme Bonelle, *Compatible Discrete Operator schemes on polyhedral meshes for elliptic and Stokes equations*, Ph.D. thesis, Université Paris-Est, Paris, France, 2014. ↑420
- [Bos88] Alain Bossavit, *Whitney forms: A class of finite elements for three-dimensional computations in electromagnetism*, IEE Proc. A Phys. Sci. Meas. Instrum. Manag. Educ. Rev. **135** (1988), no. 8, 493–500. ↑420
- [Bos98] ———, *Computational electromagnetism: variational formulations, complementarity, edge elements*, Academic Press Inc., 1998. ↑420
- [BS99] Dinshaw S. Balsara and Daniel S. Spicer, *A staggered mesh algorithm using high order Godunov fluxes to ensure solenoidal magnetic fields in magnetohydrodynamic simulations*, J. Comput. Phys. **149** (1999), no. 2, 270–292. ↑421

- [CR74] Michel Crouzeix and Pierre-Arnaud Raviart, *Conforming and nonconforming finite element methods for solving the stationary Stokes equations. I.*, Rev. Franc. Automat. Inform. Rech. Operat. **7** (1974), no. R3, 33–75. ↑448
- [DJOR16] Stéphane Dellacherie, Jonathan Jung, Pascal Omnes, and Pierre-Arnaud Raviart, *Construction of modified Godunov type schemes accurate at any Mach number for the compressible Euler system*, Math. Models Methods Appl. Sci. **26** (2016), no. 13, 2525–2615. ↑437, 448
- [DOR10] Stéphane Dellacherie, Pascal Omnes, and Felix Rieper, *The influence of cell geometry on the Godunov scheme applied to the linear wave equation*, J. Comput. Phys. **229** (2010), no. 14, 5315–5338. ↑448
- [DPD20] Daniele A. Di Pietro and Jérôme Droniou, *The Hybrid High-Order method for polytopal meshes*, Modeling, Simulation and Applications series, vol. 19, Springer, 2020. ↑420, 421
- [EG20] Alexandre Ern and Jean-Luc Guermond, *Finite elements I: Approximation and interpolation*, Texts in Applied Mathematics, vol. 72, Springer, 2020. ↑425
- [Gui09] Hervé Guillard, *On the behavior of upwind schemes in the low Mach number limit. IV: P0 approximation on triangular and tetrahedral cells*, Comput. Fluids **38** (2009), no. 10, 1969–1972. ↑420, 448
- [Hip01] Ralf Hiptmair, *Discrete Hodge operators*, Numer. Math. **90** (2001), no. 2, 265–289. ↑420
- [Hip02] ———, *Finite elements in computational electromagnetism*, Acta Numer. **11** (2002), 237–339. ↑420
- [HLX22] Qingguo Hong, Yuwen Li, and Jinchao Xu, *An extended Galerkin analysis in finite element exterior calculus*, Math. Comput. **91** (2022), no. 335, 1077–1106. ↑420
- [JP22] Jonathan Jung and Vincent Perrier, *Steady low Mach number flows: identification of the spurious mode and filtering method*, J. Comput. Phys. **468** (2022), article no. 111462. ↑437, 448
- [JP24a] ———, *Behavior of the Discontinuous Galerkin Method for Compressible Flows at Low Mach Number on Triangles and Tetrahedrons*, SIAM J. Sci. Comput. **46** (2024), no. 1, A452–A482. ↑420, 448
- [JP24b] ———, *A curl preserving finite volume scheme by space velocity enrichment. Application to the low Mach number accuracy problem*, J. Comput. Phys. **515** (2024), article no. 113252 (29 pages). ↑421
- [Lic17] Martin Werner Licht, *Complexes of discrete distributional differential forms and their homology theory*, Found. Comput. Math. **17** (2017), no. 4, 1085–1122. ↑421, 426, 447
- [MBE22] Riccardo Milani, Jérôme Bonelle, and Alexandre Ern, *Artificial compressibility methods for the incompressible Navier–Stokes equations using lowest-order face-based schemes on polytopal meshes*, Comput. Methods Appl. Math. **22** (2022), no. 1, 133–154. ↑420
- [Per24] Vincent Perrier, *Development of discontinuous Galerkin methods for hyperbolic systems that preserve a curl or a divergence constraint*, 2024, <https://arxiv.org/abs/2405.04347v1>. ↑448
- [RT77a] Pierre-Arnaud Raviart and Jean-Marie Thomas, *A mixed finite element method for 2-nd order elliptic problems*, Mathematical aspects of finite element methods. Proceedings of the conference held in Rome, December 10–12, 1975, Lecture Notes in Mathematics, vol. 606, Springer, 1977, pp. 292–315. ↑434

- [RT77b] ———, *Primal hybrid finite element methods for 2nd order elliptic equations*, Math. Comput. **31** (1977), no. 138, 391–413. ↑434
- [TD17] Maurizio Tavelli and Michael Dumbser, *A pressure-based semi-implicit space-time discontinuous Galerkin method on staggered unstructured meshes for the solution of the compressible Navier–Stokes equations at all Mach numbers*, J. Comput. Phys. **341** (2017), 341–376. ↑421

Manuscript received on 1st May 2024,
 revised on 30th October 2024,
 accepted on 2nd December 2024.

Recommended by Editors S. Vu Ngoc and N. Seguin.
 Published under license CC BY 4.0.



eISSN: 2644-9463

This journal is a member of Centre Mersenne.



Vincent PERRIER
 Team Cagire,
 INRIA Bordeaux Sud-Ouest,
 Laboratoire de Mathématiques
 et de leurs applications,
 Bâtiment IPRA,
 Université de Pau
 et des Pays de l'Adour,
 Avenue de l'Université,
 64 013 Pau Cedex (France)
 vincent.perrier@inria.fr